Journal of Extracellular Vesicles

RESEARCH ARTICLE OPEN ACCESS

Intranasal Human NSC-Derived EVs Therapy Can Restrain Inflammatory Microglial Transcriptome, and NLRP3 and cGAS-STING Signalling, in Aged Hippocampus

Leelavathi N. Madhu[1] | Maheedhar Kodali[1] | Shama Rao[1] | Sahithi Attaluri[1] | Raghavendra Upadhya[1] | Goutham Shankar[1] | Bing Shuai[1] | Yogish Somayaji[1] | Shruthi V. Ganesh[1] | Vignesh S. Kumar[2] | Jeswin E. James[1] | Padmashri A. Shetty[1] | Avery LeMaire[1] | Xiaolan Rao[1] | James J Cai[2] | Ashok K. Shetty[1]

[1]Institute for Regenerative Medicine, Department of Cell Biology and Genetics, College Station, Texas A&M University Naresh Vashisht College of Medicine, College Station, Texas, USA | [2]Department of Veterinary Integrative Biosciences, Texas A&M College of Veterinary Medicine, College Station, Texas, USA

Correspondence: Ashok K. Shetty (ash.shetty@tamu.edu)

Received: 30 May 2025 | **Revised:** 6 December 2025 | **Accepted:** 13 January 2026

Keywords: brain aging | hippocampus | GeneWalk | inflammasomes | interferon-1 signalling | mitochondrial function | microglia | mitogen-activated protein kinase signalling | neuroinflammation | scRNA-seq

ABSTRACT

Neuroinflammaging, a moderate, chronic, and sterile inflammation in the hippocampus, contributes to age-related cognitive decline. Neuroinflammaging comprises the activation of the nucleotide-binding domain, leucine-rich repeat family, and pyrin domain-containing 3 (NLRP3) inflammasomes, and the cyclic GMP-AMP synthase (cGAS)-stimulator of interferon genes (STING) pathway that triggers type 1 interferon (IFN-1) signalling. Studies have shown that extracellular vesicles from human induced pluripotent stem cell-derived neural stem cells (hiPSC-NSC-EVs) contain therapeutic miRNAs that can alleviate neuroinflammation. Therefore, this study examined the effects of late middle-aged (18-month-old) male and female C57BL6/J mice receiving two intranasal doses of hiPSC-NSC-EVs on neuroinflammaging in the hippocampus at 20.5 months of age. Compared with animals receiving vehicle treatment, the hippocampus of animals receiving hiPSC-NSC-EVs exhibited reductions in astrocyte hypertrophy, microglial clusters, and oxidative stress, along with elevated expression of antioxidant proteins and genes that maintain mitochondrial respiratory chain integrity. Moreover, hiPSC-NSC-EVs therapy decreased the levels of various proteins involved in the activation of the NLRP3 inflammasome, p38/mitogen-activated protein kinase, cGAS-STING-IFN-1, and Janus kinase and signal transducer and activator of transcription signalling pathways. Furthermore, in vitro assays using genetically engineered RAW cells and hiPSC-NSC-EVs, with or without targeted depletion of specific miRNAs, demonstrated that miRNA-30e-3p and miRNA-181a-5p, both present in hiPSC-NSC-EVs, can significantly inhibit the activation of the NLRP3 inflammasome and the STING pathway, respectively. Additionally, single-cell RNA sequencing conducted 7 days post-treatment revealed that hiPSC-NSC-EVs induce widespread transcriptomic changes in microglia, including increased expression of numerous genes that enhance oxidative phosphorylation and reduced expression of abundant genes that drive multiple proinflammatory signalling pathways. These changes mediated by hiPSC-NSC-EVs were also associated with improved cognitive and memory function. Thus, intranasal hiPSC-NSC-EVs therapy in late middle age can effectively diminish proinflammatory microglial transcriptome and signalling cascades that drive neuroinflammaging in the hippocampus, contributing to better brain function in old age.

Leelavathi N. Madhu and Maheedhar Kodali contributed equally to this work.

1 | Introduction

Improved human life expectancy over the past century has brought about longer lives and a surge in age-related ailments. Particularly, neurodegenerative diseases, including Alzheimer's disease (AD), have emerged as the leading causes of morbidity worldwide (Aunan et al. 2017; de Magalhaes et al. 2017; Gurau et al. 2018). Hence, effective strategies are urgently needed to promote successful aging, characterized by older adults maintaining better cognitive function, staying engaged in social activities, and displaying minimal signs of age-related diseases (Stambler 2017; Fan et al. 2017; Bettio et al. 2017).

Aging is associated with reduced ability to adapt to new stimuli and cognitive decline in a significant proportion of individuals (Turrini et al. 2023). Studies using animal models and human post-mortem brain tissues have suggested that cognitive impairments associated with aging are often connected to various adverse changes in the brain, particularly in the hippocampus (Bettio et al. 2017; O'Shea et al. 2016; Kodali et al. 2021). The age-related changes include increased oxidative stress, mitochondrial dysfunction, and neuroinflammaging. Neuroinflammaging, a sterile and moderate chronic neuroinflammation, increases substantially in individuals who develop neurodegenerative disorders. It is characterized by increased concentrations of reactive oxygen species (ROS), associated with mitochondrial dysfunction (Ionescu-Tucker and Cotman 2021; Bartman et al. 2024) and the activation of several neuroinflammatory signalling cascades. These include the activation of the nucleotide-binding domain leucine-rich repeat (NLR) family pyrin domain-containing 3 (NLRP3) inflammasomes (Fu et al. 2020; He et al. 2021) and the cyclic GMP-AMP synthase (cGAS) and the stimulator of interferon genes (STING) pathway, which leads to chronic type I Interferon (IFN) signalling in the aged brain (Gulen et al. 2023).

NLRP3 is predominantly expressed in microglia, the resident immune cells in the brain (Ayyubova and Madhu 2025). Activation of NLRP3 inflammasomes by danger-associated molecular patterns (DAMPs, for example, increased ROS) in microglia increases the secretion of proinflammatory cytokines, such as interleukin-1 beta (IL-1β) and IL-18. These cytokines can induce pyroptosis in neighbouring neural cells and activate the downstream p38 mitogen-activated protein kinase (p38/MAPK or pMAPK) signalling pathway via myeloid differentiation primary response 88 (Myd88) and the small GTPase rat sarcoma virus (Ras) (Kodali et al. 2023; Madhu et al. 2024). This process can contribute to a chronic state of neuroinflammation with the continuous release of higher concentrations of multiple proinflammatory cytokines. On the other hand, activation of the cGAS-STING pathway in microglia, typically triggered by double-stranded DNA (dsDNA) released from damaged cells, leads to upregulation of type-I IFN (or IFN-I) production (Gulen et al. 2023; Madhu et al. 2024), leading to the activation of Janus kinase and signal transducer and activator of transcription (JAK-STAT) signalling culminating in transcription of numerous interferon-stimulated genes (ISGs) (Gulen et al. 2023; Paul et al. 2021). Thus, it is apparent that increased oxidative stress, mitochondrial dysfunction, and microglia-mediated chronic neuroinflammation in the aged brain increase the susceptibility to develop conditions such as mild cognitive impairment (MCI) or AD (Fan et al. 2017; Bettio et al. 2017; Hedden and Gabrieli 2004). Therefore, strategies that restrain detrimental microglia-mediated inflammatory signalling cascades in the aging brain are needed to maintain better cognitive and mood function in old age. However, treatments capable of restraining such neuropathological changes associated with cognitive and memory impairments in late middle or old age have yet to be identified.

Previous studies have shown some beneficial effects of intracerebral neural stem cell (NSC) grafting in models of brain aging (Hattiangady et al. 2007; Shetty and Hattiangady 2016) and AD (Blurton-Jones et al. 2009; Ager et al. 2015). However, the benefits of NSC grafting are believed to be primarily due to bystander effects (i.e., paracrine actions of their secretome), which include antiinflammatory, neuroprotective, and neuroreparative activity (Hattiangady and Shetty 2012; Eckert et al. 2015). From this perspective, extracellular vesicles (EVs) from human induced pluripotent stem cell (hiPSC)-derived NSCs, which retain most of the therapeutic effects of parental cells, have attracted attention for developing cell-free therapies. Also, intranasally (IN) administered hiPSC-NSC-EVs efficiently target microglia and astrocytes throughout the brain (Upadhya et al. 2020; Attaluri et al. 2023) and have been shown to induce beneficial transcriptomic changes in conditions such as AD (Madhu et al. 2024). Furthermore, the cargo (miRNAs and proteins) carried by these EVs has been previously validated for its ability to mediate antioxidant, antiinflammatory, and neuroprotective effects using in vitro and in vivo models (Madhu et al. 2024; Upadhya et al. 2020; Upadhya et al. 2022; Ayyubova et al. 2023; Rao et al. 2025). Therefore, using a mouse model, this study investigated whether IN administration of hiPSC-NSC-EVs in late middle age can significantly reduce oxidative stress and curb microglia-mediated neuroinflammaging in the hippocampus. The results provide new evidence that hiPSC-NSC-EVs therapy in late middle age can diminish the proinflammatory transcriptome of microglia, leading to reductions in oxidative stress, mitochondrial dysfunction, and neuroinflammaging associated with better cognitive and memory function in old age. Robust antiinflammatory effects of hiPSC-NSC-EVs were apparent from diminished activation of signalling cascades such as the NLRP3, p38/MAPK, cGAS-STING, JAK-STAT, and IFN-1 pathways in the aged hippocampus.

2 | Materials and Methods

2.1 | hiPSC-Derived NSC Cultures, Purification and Characterization of hiPSC-NSC-EVs

The procedures for generating NSCs from hiPSCs (Wisconsin International Stem Cell Bank (IMR90-4), passaging of hiPSC-NSCs, isolation of EVs from passage 11 (P11) hiPSC-NSCs, and characterization of the number, size, and markers of hiPSC-NSC-EVs are detailed in our previous reports (Madhu et al. 2024; Upadhya et al. 2020; Upadhya et al. 2022) and the supplemental file.

2.2 | Animals and Study Design

The study comprised two cohorts of C57BL/6 mice: young adult (3 months old) and late middle-aged (18 months old). We chose 18 months old mice, as this mouse age is approximately equivalent

to a 60-year-old human (Dutta and Sengupta 2016). The mice were purchased from Jackson Laboratories (Bar Harbor, Maine, USA) and housed with ad libitum access to food (4% fat diet) and water ($n = 131$; 61 males and 70 females). The Institutional Animal Care and Use Committee of Texas A&M University approved all studies conducted in this investigation. Male and female late middle-aged mice were randomly assigned to either the vehicle group (aged-Veh; $n = 31$ [13 males and 18 females]) or the EVs group (aged-EVs; $n = 30$ [12 males and 18 females]) for long-term studies. For single-cell RNA sequencing (sc-RNA-seq) studies on microglia, additional late middle aged male mice were recruited to the aged-Veh and aged-EVs groups ($n = 1$/group). Furthermore, additional groups of 3-month-old mice ($n = 28$, 14 males and 14 females) and 18-month-old mice ($n = 32$, 16 males and 16 females) underwent neurobehavioral testing to assess cognitive status at 18 months of age, the timepoint chosen for the hiPSC-NSC-EVs treatment intervention in the study. Additionally, late-middle-aged mice were used to evaluate the incorporation of IN-administered PKH-26-labeled hiPSC-NSC-EVs into neural cells across various brain regions ($n = 8$; four males and four females). Figure 1G details the study design, including the time points for the IN-administration of hiPSC-NSC-EVs, neurobehavioral tests, and euthanasia.

The animals in the aged-Veh or aged-EVs group for long-term studies received two doses of the vehicle or the hiPSC-NSC-EVs treatment (12×10^9 EVs, ~25 µg total protein), with each dose administered 2 weeks apart. The selection of dose was based on the results of our previous studies to reduce neuroinflammation in a lipopolysaccharide-induced peripheral inflammation model using young C57BL6 mice (Ayyubova et al. 2023). One month after the last dose, all animals underwent neurobehavioral testing. Following cognitive assessments, subgroups of animals were perfused with 4% paraformaldehyde, and collected brain tissues were processed for immunohistochemical studies ($n = 6$–8/group) or euthanized to harvest fresh brain tissues for biochemical and molecular biological studies ($n = 6$–8/group). The investigators conducting the behavioural tests and those performing immunohistochemical, immunofluorescence, biochemical, or molecular biological analyses were blinded to the group identities of animals or samples. Late middle-aged male and female mice recruited to biodistribution studies were euthanized 6 h after receiving an IN administration of hiPSC-NSC-EVs labelled with PKH-26 (4×10^9 EVs) to confirm the biodistribution of EVs into neural cells across various regions of the brain. Late middle-aged male mice recruited to sc-RNA-seq studies were euthanized 7 days after receiving a single IN dose of hiPSC-NSC-EVs (12×10^9 EVs) to isolate live microglia.

2.3 | Evaluation of the Interaction of IN-Administered hiPSC-NSC-EVs With Microglia and Astrocytes

The animals were perfused with 4% paraformaldehyde 6 h after an IN administration of PKH-26-labeled hiPSC-NSC-EVs to visualize the interaction of IN-administered PKH-26-labeled hiPSC-NSC-EVs (fluorescing red) with neural cells. Thirty-micrometre-thick serial sections were cut using a cryostat, and every 15th section through the entire forebrain from each animal ($n = 4$/sex) was processed for ionized calcium-binding adaptor molecule 1 (IBA-1) or glial fibrillary acidic protein (GFAP) immunofluorescence to confirm the interaction or association of PKH-26-labeled hiPSC-NSC-EVs with microglia and astrocytes. The primary and secondary antibodies comprised anti-goat IBA-1 (1:1000, Abcam, Cambridge, UK), rabbit anti-GFAP (1:2000, Dako, Glostrup, Denmark), donkey anti-goat IgG conjugated to Alexa Fluor 488 (1:200, Invitrogen, Waltham, MA, USA), and donkey anti-rabbit IgG conjugated to Alexa Fluor 488 (1:200, Invitrogen). The supplemental file comprises the methods employed for IBA-1 and GFAP immunofluorescence.

2.4 | Analyses of Cognitive Function

The study employed two neurobehavioral tests to measure cognitive function. A novel object recognition test (NORT) was used to investigate the competence for recognition memory, which relies on an interaction between the hippocampus and the perirhinal cortex (Aggleton et al. 2010). Furthermore, an object location test (OLT) assessed the proficiency of animals in discerning subtle changes in their immediate environment, a cognitive function dependent on the integrity of the hippocampus (Barker and Warburton 2011). The detailed protocols used for OFT, NORT, and OLT are available in our previous reports (Kodali et al. 2023; Madhu et al. 2024; Hattiangady et al. 2014; Shetty et al. 2020) and in the supplementary file. In animals receiving vehicle or hiPSC-NSC-EVs treatment, these tests were performed between 19.5 and 20.5 months of age, along with age-matched naïve control animals.

2.5 | Tissue Processing, and Immunohistochemical, Immunofluorescence, and Biochemical Studies

After the completion of cognitive tests (i.e., at 20.5 months of age), the animals were euthanized, and the brain tissues were processed for immunohistochemical and biochemical analyses. The detailed methods employed for brain tissue collection, processing, immunohistochemistry, single/dual/triple immunofluorescence, and biochemical and molecular biological studies are available in our previous reports (Kodali et al. 2023; Madhu et al. 2024; Rao et al. 2008; Hattiangady et al. 2011) and the supplemental file.

2.6 | Quantification of Number and Clusters of Microglia in the Hippocampus

The microglial clusters and microglial numbers in the hippocampus of male and female mice belonging to aged-Veh and aged-EVs groups ($n = 6$/sex/group) were measured, using every 20th section through the hippocampus. Microglial numbers were measured via stereological counting of IBA1+ cells using the optical fractionator method in the StereoInvestigator system (Microbrightfield, Williston, Vermont, USA). They were expressed as the number per 0.1 mm^3 of hippocampal volume. The detailed stereological methods employed are described in our earlier reports (Rao et al. 2006, 2007; Kodali et al. 2016). We assessed the total number of microglial clusters for the hippocampus by counting every cluster (accumulation of three or more microglia) in serial sections (every 20th through the entire

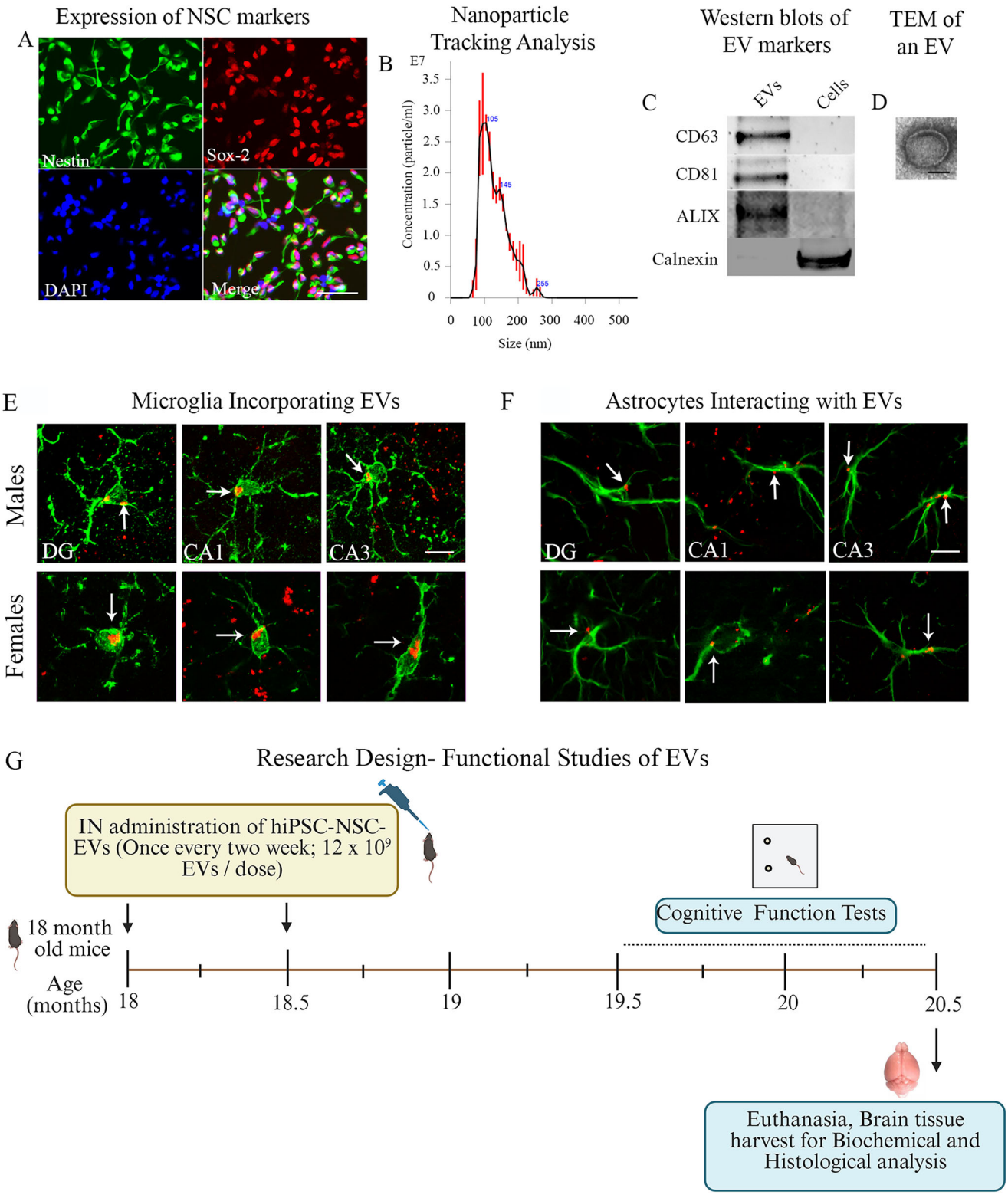

FIGURE 1 | **Characterization of extracellular vesicles (EVs) from human induced pluripotent stem cell-derived neural stem cells (hiPSC-NSCs), assessment of hiPSC-NSC-EVs biodistribution in the hippocampus and cerebral cortex of late middle-aged mice, and timeline of in vivo experiments**. Image A illustrates that all cells in passage 11 NSCs derived from hiPSCs express NSC markers Nestin and Sox-2. Graph B shows the size and number of hiPSC-NSC-EVs measured with a NanoSight. The blots in C demonstrate EV-specific proteins CD63, CD81, and ALIX, and the absence of the deep cellular protein calnexin in hiPSC-NSC-EVs. The image in D shows the morphology and size of hiPSC-NSC-EVs as visualized by transmission electron microscopy. scale bars, A = 100 μm, D = 50 nm. Figure E illustrates the incorporation of EVs into IBA-1+ microglia in different hippocampal subregions (DG, CA1, and CA3) from male and female mice. Figure F illustrates the interaction of EVs with GFAP+ astrocytes in hippocampal subregions (DG, CA1, and CA3) from male and female mice. Scale bar, E-F = 10 μm. Panel G illustrates the experimental design for long-term experiments showing the time points of hiPSC-NSC-EVs treatment, cognitive and mood function tests, euthanasia, and brain tissue harvest in late middle-aged male and female mice.

hippocampus and then extrapolating the average number per section for the total number of sections through the hippocampus ($n = 6$/group).

2.7 | Measurement of Oxidative Stress Markers, Antioxidants, and Nuclear Factor Erythroid 2-Related Factor 2 (NRF2)

Commercially available kits were employed to measure oxidative stress markers malondialdehyde (MDA) and protein carbonyls (PC) (Cayman Chemicals, Arbor, MI, USA), and NRF2 (Signosis, Santa Clara, CA, USA), in hippocampal lysates ($n = 6$/sex/group). We followed the manufacturer's instructions for performing these assays. Furthermore, to evaluate antioxidant status in the hippocampus, we measured superoxide dismutase (SOD) and catalase (CAT) concentrations in hippocampal lysates. The total protein concentration in the various tissue lysates was determined using a Pierce BCA Protein Assay Kit from ThermoFisher Scientific (Waltham, MA, USA). The concentrations of markers were normalized to the total protein content in their respective tissue lysates.

2.8 | Measurement of Genes Linked to Mitochondrial Respiratory Chain

We analysed the expression of many genes regulating the mitochondrial respiratory chain in the hippocampus, using specific primers purchased from GeneCopoeia (Rockville, MD, USA) ($n = 6$/sex/group). The measured genes encoding proteins relevant to the mitochondrial electron transport chain and oxidative phosphorylation include the *Ndufs6* and *Ndufs7* (Complex I), *Sdha* and *Sdhb* (Complex II), *Bcs1l* and *Cyc1* (Complex III); *Cox4i2* and *Cox7b* (Complex IV), *Atp6ap1* (Complex V) and *Slc25a10* (a gene encoding the mitochondrial dicarboxylate carrier protein). *Gapdh* was used as a housekeeping gene. The 2ˆdelta-delta Ct (2^{ddCT}) values for each gene were compared across different groups. All gene names mentioned in this manuscript have been expanded in the supplemental file (Table S1).

2.9 | Measurement of NLRP3 Inflammasome Genes, and NLRP3-ASC Inflammasome Complexes in Microglia

We first performed qRT-PCR to measure the expression of genes *Nlrp3, Pycard, Casp1, Il1β*, and *Il18*. Then, to determine the extent of NLRP3-apoptosis-associated speck-like protein containing a caspase recruitment domain (ASC) inflammasome complexes and the percentages of microglia presenting NLRP3-ASC complexes, the brain tissue sections were processed for triple immunofluorescence to visualize IBA-1, NLRP3, and ASC in microglia. Using Z-section analysis in a Nikon confocal microscope or a Leica THUNDER 3D Imager, the number of NLRP3-ASC inflammasome complexes per unit area (~216 μm^2) and the percentages of IBA-1+ microglia co-expressing NLRP3-ASC inflammasome complexes were measured. For these quantifications, data collected from individual subfields of the hippocampus (DG, CA1, and CA3) were pooled across three sections/animal ($n = 6$/sex/group) (Kodali et al. 2023; Madhu et al. 2024; Ayyubova et al. 2023). The supplemental file comprises information on the antibodies employed and detailed methods.

2.10 | Quantification of Markers Involved in the Activation of NLRP3 Inflammasome and p38/MAPK Signalling Cascades

The hippocampal lysates from male and female mice were processed to quantify the concentrations of various markers of NLRP3 inflammasome activation and p38/MAPK signalling ($n = 6$/group), using commercially available individual enzyme-linked immunosorbent assay (ELISA) kits, as detailed in our previous studies (Kodali et al. 2023; Madhu et al. 2024, 2021). These include assay kits for (1) nuclear subunit of Nuclear factor kappa B (NF-kB p65; Aviva Systems Biology, San Diego, CA, USA), (2) NLRP3 (Abcam), (3) ASC (MyBioSource, San Diego, CA, USA), (4) cleaved caspase-1 (Abcam), (5) IL-18 (R&D Systems, Minneapolis, MN, USA), (6) IL-1β (R&D Systems, (7) MyD88 (Aviva Systems Biology), (8) Ras, (MyBioSource), (9) p38 MAPK (Cell Signalling, Danvers, MA, USA), (10) activator protein-1 (AP-1, Novus Biologicals, Centennial, CO; USA), and (11) tumour necrosis factor-alpha (TNF-α, R&D systems), and (12) IL-8 (Biomatik, Wilmington, DE, USA). The concentrations of individual proteins were normalized to 1 mg of total protein in hippocampal lysates.

2.11 | Quantification of Markers Associated With Activation of cGAS-STING Signalling Pathway

We measured the concentrations of (1) c-GAS (Cell Signalling, Danvers, MA, USA), (2) p-STING (Cell Signalling), (3) phosphorylated TANK-binding kinase-1 (p-TBK-1), (4) phosphorylated interferon regulatory factor 3 (p-IRF3; ABclonal, Woburn, MA, USA), and (5) IFN-α (LS-BIO, Lynnwood, WA, USA) in hippocampal lysates of male and female mice (Madhu et al. 2024). Since the activation of the cGAS-STING pathway stimulates the JAK-STAT signalling (Chen et al. 2024), we also measured concentrations of the phosphorylated JAK1 and JAK2 and the phosphorylated STAT1 and STAT3 in the hippocampal lysates of male and female aged mice. In addition, we performed qRT-PCR to measure the expression of ISG genes *Irf1*, *Icam1, Cd47, Irf5, Alcam, Irf7, Ifnγ*, and *Tnf* in RNA samples isolated from hippocampus tissue of aged Veh and aged-EVs groups of male and female mice.

2.12 | Depletion of miR-30e-3p and miR-181a-5p in hiPSC-NSCs via Transfection With Antagomirs

Previous studies have suggested that miR-30e-3p can inhibit NLRP3, by binding to the 3' untranslated region (3'UTR) of NLRP3 mRNA (Li et al. 2018), and miR-181a-5p can inhibit STING by directly binding to its mRNA (Bustos et al. 2023), resulting in decreased expression of NLRP3 and STING proteins, respectively. Since both miR-30e-3p and miR-181a-5p are enriched in hiPSC-NSC-EVs, we investigated whether these miRs play significant roles in hiPSC-NSC-EVs-mediated inhibition of the activation of NLRP3 inflammasome and c-GAS-STING signalling. We first generated hiPSC-NSC-EVs with diminished expression of miR-30e-3p or miR-181a-5p. For this, P11 hiPSC-NSCs with 60%

confluency in 6-well plates were transfected with 100 nM miR-30e-3p or 181a-5p inhibitor (AUM Biotech, Philadelphia, PA, USA) using Lipofectamine 2000 transfection reagent (Invitrogen) in Opti-MEM media (ThermoFisher Scientific). Four hours later, Opti-MEM media were replaced with the NSC media, and cultures were maintained for an additional 48 h with fresh NSC media. Next, spent media from cultures of transfected hiPSC-NSCs and their non-transfected counterparts were used to isolate EVs, as described in our earlier report (Upadhya et al. 2022), and qRT-PCR was employed to measure the levels of miR-30e-3p or miR-181a-5p. For this, total RNA from NSC-EVs was first isolated using the SeraMir Exosome RNA amplification kit (System Biosciences), and the miRCURY LNA RT Kit (Qiagen) was then used to convert 5 ng/μL of total RNA into cDNA. Next, miRCURY LNA miRNA SYBR Green PCR kit (Qiagen) and miRCURY LNA miRNA PCR assay primer mix (Qiagen) were employed to measure miRNA levels. Later, significantly depleted miR-30e-3p or miR-181a-5p levels in EVs generated from transfected hiPSC-NSCs were confirmed by comparing them with levels in EVs from non-transfected hiPSC-NSCs.

2.13 | Assessing the Effects of hiPSC-NSC-EVs With Depleted miR-30e-3p on NLRP3 Inflammasome Activation

To investigate the mechanism by which hiPSC-NSC-EVs suppress NLRP3 inflammasome activation, we performed an in vitro assay using RAW-ASC cells (InvivoGen, San Diego, CA, USA). These cells, derived from the murine RAW 264.7 macrophage line that are naturally ASC-deficient, were stably transfected with the murine ASC gene. RAW-ASC cells secrete IL-1β upon activation of canonical (e.g., NLRP3) or non-canonical (e.g., caspase-11) inflammasomes. For this, we first induced NLRP3 activation using nigericin, a well-characterized ionophore that promotes NLRP3 assembly with ASC adaptor protein and pro-caspase-1 to form an inflammasome complex. We next measured the concentrations of end products of NLRP3 inflammasome activation, the proinflammatory cytokines IL-1β and IL-18 in cells and culture media. Briefly, RAW-ASC cells were seeded at a density of 2×10^5 cells/well in a 24-well plate and cultured for 24 h in DMEM supplemented with 10% FBS and phenol red. Next, the media was replaced with serum-free DMEM containing 10 μM nigericin. Four hours later, the RAW ASC cultures were treated with 0.6×10^9 hiPSC-NSC-EVs depleted with miR-30e-3p or naive hiPSC-NSC-EVs ($n = 3$ wells/group). After 20 h of treatment, the culture media and cells were collected to measure IL-1β and IL-18 levels using ELISA kits (R&D Systems).

2.14 | Assessing the Effects of hiPSC-NSC-EVs With Depleted miR-181a-5p on STING Activation

To understand the mechanism through which hiPSC-NSC-EVs reduce STING activation, we performed an in vitro assay using RAW-Lucia ISG cells (InvivoGen, San Diego, CA, USA). RAW-Lucia ISG cells express multiple pattern recognition receptors (PRRs), including the cyclic dinucleotide sensor STING. Activation of PRRs induces production of type 1 IFNs through the TBK-1-IRF3 axis. RAW-Lucia ISG cells also express the secreted Lucia luciferase reporter gene under the control of an ISG54 minimal promoter in conjunction with five IFN-stimulated response elements (ISRE). Hence, IRF3 activation in these cells can be determined by measuring the activity of the Lucia luciferase reporter. In this experiment, we used 2',3' cGAMP, which polymerized STING, and led to the activation of the TBK-1-IRF3 axis and the production of type 1 IFNs. We assessed IRF3 activation by measuring luciferase activity in the Lucia reporter via luminescence and IFNα production by ELISA. Briefly, RAW-Lucia^{TM}-ISG cells were seeded in a 24-well plate at a density of 2×10^5 cells/well in DMEM medium containing 10% FBS. After 24 h, the media was replaced with serum-free DMEM (phenol red-free) containing 5 μM 2′,3′-cGAMP to activate STING. Four hours later, cultures were incubated with 0.6×10^9 hiPSC-NSC-EVs depleted with miR-181a-5p or naive hiPSC-NSC-EVs ($n = 6$ wells/group). Twenty hours later, supernatants from cultures were collected for measurement of luciferase activity, and cells were processed for IFNα quantification by ELISA (Ray Biotech). Lucia luciferase activity was measured from each culture by mixing 20 μL of the culture supernatant with 50 μL of the QANTI-Luc^{TM} 4 (1X) reagent in a 96-well white (opaque) plate. After gentle tapping, the luminescence was immediately recorded using a luminometer. The relative luminescence values were compared across the experimental groups.

2.15 | Single-Cell RNA Sequencing (scRNA-seq) of Microglia

Late middle-aged male mice (18 months old) were euthanized 7 days after administration of 12×10^9 hiPSC-NSC-EVs or Veh ($n = 1$/group). Fresh brains were immediately harvested and processed for the isolation of live microglia. Brain tissues were dissociated into single-cell suspensions using the gentleMACS Tissue Dissociator (Miltenyi Biotec, Gaithersburg, MD, USA). Microglia were isolated via magnetic-activated cell sorting (MACS) using CD11b-conjugated microbeads (Miltenyi Biotec) and MACS Separators. Following live cell analysis and quality control measures, the live microglia were processed for scRNA-seq using the 10× Genomics Chromium GEM-X platform, targeting approximately 10,000 microglia per sample. Library preparation and sequencing were performed at the Texas A&M Institute for Genome Sciences and Society (TIGSS). Individually barcoded libraries were pooled and sequenced on a NextSeq 2000 system using a P4 100-cycle flow cell (Illumina, San Diego, CA, USA) according to the manufacturer's instructions. The differentially expressed gene analysis was performed using scGEAToolbox (Cai 2019). The detailed methods for sequence alignment, filtering, and enrichment pathway analysis are provided in the supplementary file.

Next, we used the SelectCellByClass function in scGEAToolbox to extract microglial clusters from gene expression profiles in the SingleCellExperiment (SCE) object. The resulting cluster-specific SCE objects were then subjected to differential gene expression analysis, with detailed analysis provided in the supplementary materials. Furthermore, we performed GeneWalk analysis using the differentially expressed genes (DEGs) between the aged-Veh and aged-EVs groups. GeneWalk identifies relevant biological functions for genes by performing random walks on a knowledge graph that integrates gene networks with Gene Ontology (GO) annotations (da Rocha et al. 2025). Mouse genes were

first mapped to human orthologs, and all reactions between these orthologs were extracted from the knowledge base and automatically assembled into a gene network. Then, GO and annotations were added to these networks, resulting in the complete GeneWalk network. GeneWalk automatically identifies regulator genes (those with high connectivity to other input genes and a high fraction of relevant GO annotations) and moonlighting genes (those with many GO annotations but a low fraction of relevant ones). Moreover, since GeneWalk uses an adjusted p value < 0.1 for these classifications, we further filtered the results to retain only genes with an adjusted p value < 0.055. To further refine the set of strong regulator candidates, we applied two additional criteria: a fraction of relevant GO terms ≥ 0.7 and gene connectivity ≥ 75 (a connectivity of 100+ indicates a hub gene). Application of these filters excluded all moonlighting genes and a few regulator genes. We also removed GO terms in the cellular component domain. Finally, a GeneWalk scatterplot was generated that retained all genes with <250 connections.

2.16 | Power Analyses and Statistics

The numbers of animals per group for neurobehavioral and brain tissue studies were determined via power analysis using data from our previous studies, the details of which are provided in the supplemental file. Statistical analyses were done using Prism software version 10.2. Within-group comparisons in neurobehavioral tests and two-group comparisons utilized either a two-tailed, unpaired Student's t-test or a Mann–Whitney U-test, depending on whether the datasets had significantly different standard deviations. The variability across individual animals was comparable between the Aged-Veh and Aged-EVs groups, as indicated by the normality test comparing standard deviations between groups. A p value of less than 0.05 was considered statistically significant in all tests. A two-way ANOVA followed by Tukey's multiple comparisons post-hoc tests was employed to assess sex-dependent effects and the interaction between sex and hiPSC-NSC-EVs treatment.

3 | Results

3.1 | Attributes of hiPSC-NSC-EVs Employed in the Study

The P11 hiPSC-NSC cultures employed in the study exclusively comprised NSCs, as all cells expressed the NSC markers nestin and Sox-2 (Figure 1A). EVs isolated from these cultures using anion-exchange and size-exclusion chromatography had a mean size of 130.9 nm (Figure 1B). These EVs exhibited specific markers, such as the tetraspanins CD63 and CD81, and ALIX. However, they did not contain the cytoplasmic marker calnexin, which is present in hiPSC-NSCs (Figures 1C and S1). Additionally, transmission electron microscopy confirmed the presence of double-membrane-bound vesicles in the EV preparations (Figure 1D). Our previous study demonstrated that various protein and miRNA cargoes carried by these hiPSC-NSC-derived EVs exhibit antioxidant, anti-inflammatory, and neuroprotective properties (Upadhya et al. 2020, 2022).

3.2 | Biodistribution of IN-Administered hiPSC-NSC-EVs in the Brain of Late Middle-Aged Mice

The biodistribution of IN-administered PKH-26-labeled hiPSC-NSC-EVs was examined in multiple brain regions using markers of neural cells at 6 h post-administration (Figure 1E, F) in both male and female mice. Such analysis revealed that hiPSC-NSC-EVs permeated virtually all brain regions within 6 h post-administration, as demonstrated in our earlier studies for naïve mice (Upadhya et al. 2020) and 5× Familial AD (5×FAD) mice (Attaluri et al. 2023). In all brain regions, EVs were taken up by microglia and neurons. EVs were also seen interacting with the cell membranes of astrocytes and oligodendrocytes. As this study focused on hiPSC-NSC-EVs treatment-mediated changes in microglia and astrocytes, examples of hiPSC-NSC-EVs incorporation by IBA-1+ microglia and the interaction of hiPSC-NSC-EVs with the plasma membrane of soma and processes of GFAP+ astrocytes in the hippocampal subregions (DG, CA1, and CA3) are illustrated for both male and female mice (Figure 1E, F). hiPSC-NSC-EVs incorporation by IBA-1+ microglia and the interaction of hiPSC-NSC-EVs with GFAP+ astrocytes in other brain regions are illustrated in the Supplemental File (Figure S2). Overall, the biodistribution of IN-administered hiPSC-NSC-EVs in late middle-aged mice mirrored the distribution pattern observed in young adult mice (Upadhya et al. 2020; Attaluri et al. 2023).

3.3 | hiPSC-NSC-EVs Reduced Astrocyte Hypertrophy in the Hippocampus

An evaluation of the morphology of GFAP+ astrocytes in the hippocampus suggested that hypertrophy of astrocytes decreased in the aged-EVs group compared to the aged-Veh group. Representative images from the CA3 subfield of the hippocampus from male and female aged-Veh and aged-EVs groups are illustrated (Figure 2A–D). Measurements of the area fraction of GFAP+ astrocytic elements in the hippocampus, using ImageJ, confirmed that both male and female subjects in the aged-EVs group exhibited lower levels of GFAP+ structures than their counterparts in the aged-Veh group ($p < 0.0001$; Figure 2E, F). A two-way ANOVA revealed sex-dependent differences in astrocyte hypertrophy within the aged-Veh group, with male mice exhibiting higher levels than female mice ($p < 0.05$). However, an analysis of the interaction between sex and EVs treatment demonstrated that both male and female mice responded positively to EVs treatment ($p < 0.05$; Table S2). Thus, treatment with hiPSC-NSC-EVs in late middle age can reduce astrocyte hypertrophy in the aged hippocampus.

3.4 | hiPSC-NSC-EVs Reduced Microglial Numbers and Clusters in the Hippocampus

Analysis of the distribution of IBA-1+ microglia in the hippocampus suggested a comparable density of microglia in the aged-EVs group compared to the aged-Veh group. Representative images from the CA3 subfield of the hippocampus from male and female aged-Veh and aged-EVs groups are illustrated (Figure 2G–J). Stereological quantification of the microglial

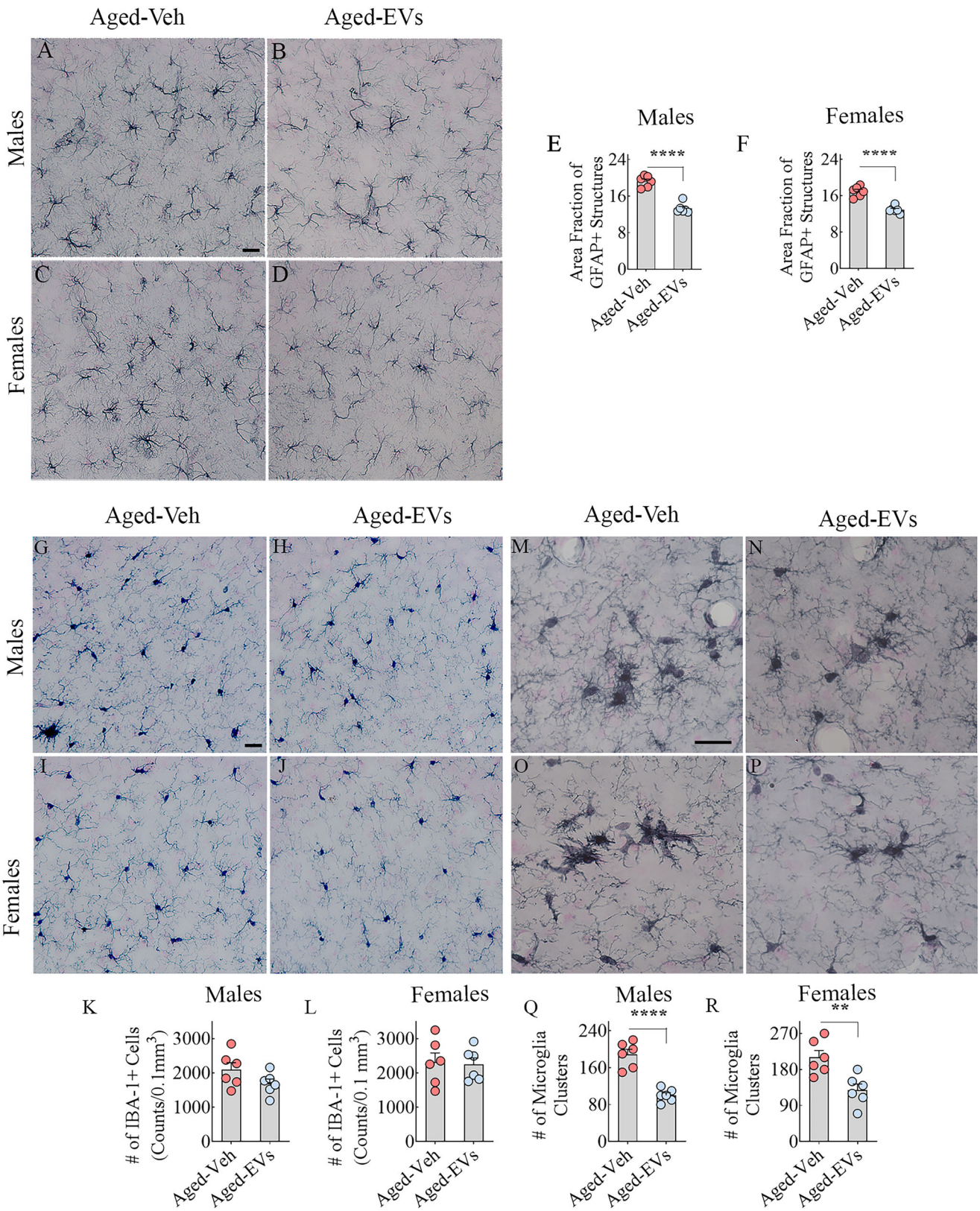

FIGURE 2 | Intranasal administration of extracellular vesicles from human induced pluripotent stem cell-derived neural stem cells (hiPSC-NSC-EVs) to late middle-aged mice reduced hypertrophy of astrocytes and microglial clusters. Figures A–D illustrate the representative images of GFAP+ astrocytes from aged-Veh (A, C) and aged-EVs (B, D) groups for males (A-B) and females (C-D). Bar charts E and F compare the area fraction (AF) of GFAP+ structures in the hippocampus of males (E) and females (F) between the aged-Veh and aged-EV groups. Figures G-J illustrate the representative images of IBA-1+ microglia from aged-Veh (G, I) and aged-EVs (H, J) groups for males (G-H) and females (I-J). Bar charts K and L compare the density of IBA-1+ microglia per 0.1 mm^3 in the hippocampus in males (K) and females (L) between the aged-Veh and aged-EV groups. Figures M-P illustrate the representative images of microglia clusters from aged-Veh (M, O) and aged-EVs (N, P) groups for males (M-N) and females

numbers per unit volume of the hippocampus confirmed that both male and female mice from the aged-Veh and aged-EVs group displayed comparable densities of IBA-1+ microglia in the hippocampus ($p > 0.05$; Figure 2K–L), implying that EVs treatment did not alter the microglial number. However, an examination of microglial clusters comprising hypertrophied microglia, indicative of disease-associated microglial phenotypes (Silvin et al. 2022; Antignano et al. 2023), in the hippocampus revealed lower levels in the aged-EVs group than in the aged-Veh group. Representative examples from the dentate molecular layer of male and female mice in the aged-Veh and aged-EVs groups are shown (Figure 2M–P). Quantification of these microglial clusters along the septo-temporal axis of the hippocampus confirmed that both male and female mice in the aged-EVs group had fewer microglial clusters compared to those in the aged-Veh group ($p < 0.01$–0.0001, Figure 2Q–R). A two-way ANOVA analysis revealed neither sex-dependent differences in microglial numbers or clusters in aged-Veh and aged-EVs groups nor interactions between sex and hiPSC-NSC-EVs treatment (Table S2). Thus, hiPSC-NSC-EVs treatment in late middle age can reduce disease-associated microglia phenotypes in the aged hippocampus.

3.5 | hiPSC-NSC-EVs Reduced Oxidative Stress With Enhanced NRF2 in the Hippocampus

Proficiency of hiPSC-NSC-EVs to reduce oxidative stress was investigated by measuring markers of oxidative stress (MDA and PCs), the master regulator of oxidative stress (NRF2), and antioxidants (SOD and CAT). Compared to the aged-Veh group, both males and females in the aged-EVs group displayed reduced concentrations of MDA and PCs ($p < 0.01$–0.0001, Figure 3A, B, F–G), increased concentrations of NRF-2 and SOD ($p < 0.01$, Figure 3C, D, H–I). The concentration of CAT in the aged-EVs group was increased in females ($p < 0.01$, Figure 3J) but not in males ($p > 0.05$, Figure 3E). Two-way ANOVA analyses showed neither sex-dependent differences in the concentrations of MDA, PCs, NRF2, and SOD in aged-Veh and aged-EVs groups nor interactions between sex and hiPSC-NSC-EVs treatment. However, CAT concentration was sex-dependent in the aged-EVs group, with females exhibiting higher CAT concentration ($p < 0.01$; Table S2), and the interaction between sex and EVs treatment revealed that only female mice responded positively to EVs treatment ($p < 0.01$; Table S2). Thus, hiPSC-NSC-EVs treatment in late middle age can reduce oxidative stress in the aged hippocampus.

3.6 | hiPSC-NSC-EVs Enhanced Mitochondrial Respiratory Chain Gene Expression in the Hippocampus

The competence of hiPSC-NSC-EVs to enhance the expression of genes linked to the mitochondrial respiratory chain was investigated in the hippocampus, as increased oxidative stress damages mitochondria, thereby impairing mitochondrial respiratory chain activity (Stefanatos and Sanz 2018). The measured genes comprised those linked to the activity of complex I *(Ndufs6, Ndufs7)*, complex II *(Sdha, Sdhb)*, complex III *(Cyc1, Bcs1l)*, complex IV *(Cox7b, Cox4i2)*, and complex V *(Slc25a1, Atp6ap1)* (Figure 3K, V). Compared to the aged-Veh group, males in the aged-EVs group displayed significantly increased expression of many genes, including *Ndufs6, Ndufs7, Sdha, Sdhb, Cyc1, Cox4i2, Slc25a1*, and *Atp6ap1* ($p < 0.05$–0.01, Figure 3L–P, S–U). Females in the aged-EVs groups showed a similar trend but with fewer genes *(Ndufs6, Ndufs7, Cyc1, Cox4i2, Slc25a1)* showing significantly increased expression than their counterparts in the aged-Veh group ($p < 0.05$–0.001, Figure 3W–X, AA, AD–AE). Two-way ANOVA analyses showed neither sex-dependent differences in aged-Veh and aged-EVs groups nor interactions between sex and hiPSC-NSC-EVs treatment for most of the measured genes linked to the mitochondrial respiratory chain ($p > 0.05$, Table S2). However, the expression of *Ndufs6* was sex-dependent in the aged-EVs group, with females exhibiting an increased expression ($p < 0.05$, Table S1), but analysis of the interaction between sex and EVs treatment revealed that *Ndufs6* expression in both male and female mice responded positively to EVs treatment ($p < 0.01$; Table S2). Thus, hiPSC-NSC-EVs treatment in late middle-aged male and female mice enhanced mitochondrial respiratory chain gene expression in the aged hippocampus.

3.7 | hiPSC-NSC-EVs Restrained the Activation of NLRP3 Inflammasome Cascade in the Hippocampus

Proficiency of hiPSC-NSC-EVs to restrain the activation of NLRP3 inflammasomes was examined by three measures, which include quantification of (1) the expression of associated genes such as *Nlrp3, Pycard, Casp1, Il1β, Il18* (Figure 4A–L), (2) percentages of microglia exhibiting NLRP3-ASC complexes (Figure 4M–Z), and (3) the concentrations of proteins involved in their activation, including NF-kB-p65, NLRP3, ASC, Cleaved Caspase-1, IL-18, and IL-1β, (Figure 4AA–AL). Compared with the aged-Veh group, males in the aged-EVs group showed decreased expression of all measured genes, with *Nlrp3, Pycard*, and *Il18* showing significant declines ($p < 0.05$–0.001; Figure 4B–C, E). Females in the aged-EVs groups showed a similar trend, with *Nlrp3* and *il18* showing significantly decreased expression compared to their counterparts in the aged-Veh group ($p < 0.05$, Figure 4H, K). Next, the extent of NLRP3-ASC inflammasome complexes within microglia of the hippocampus was examined via triple immunofluorescence for NLRP3, ASC, and IBA-1 and Z-section analysis (Figure 4M–Y). Compared with the aged-Veh group, both males and females in the aged-EVs group showed lower percentages of microglia expressing NLRP3-ASC inflammasome complexes ($p < 0.01$, Figure 4S, Z).

To corroborate the above findings, the concentrations of proteins involved in NLRP3 inflammasome activation were measured. Compared with the aged-Veh group, males in the aged-EVs group showed decreased concentrations of all measured proteins, with NF-kB-p65, NLRP3, ASC, and IL-18 showing significant declines ($p < 0.05$-0.001; Figure 4AA–AC, AE). Females in the aged-

(O-P). Bar charts Q-R compare the number of microglia clusters in the hippocampus of males (Q) and females (R) between the aged-Veh and aged-EV groups. Scale bar, A-D, G-J, M-P = 25 μm **, $p < 0.01$; and ****, $p < 0.0001$.

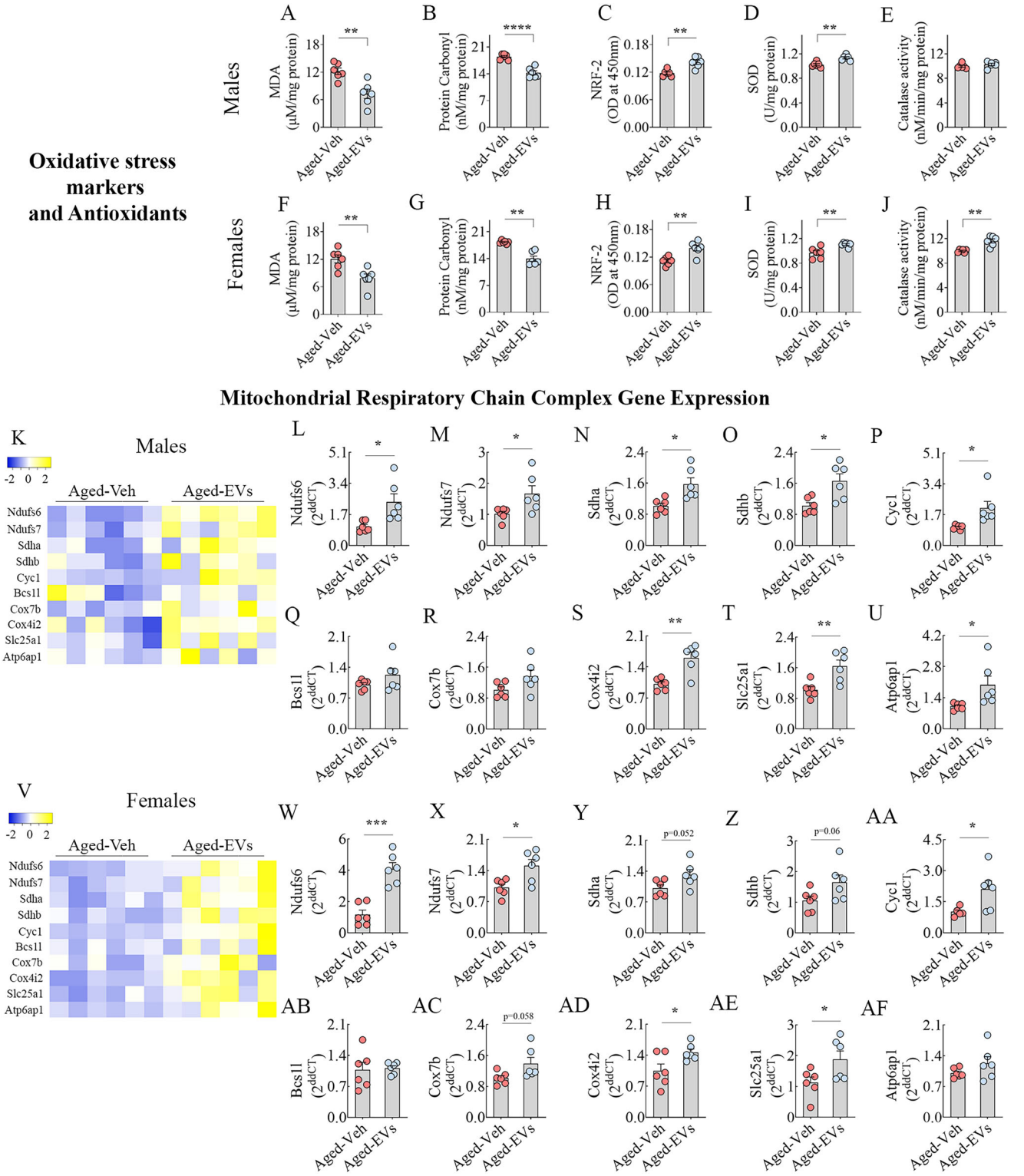

FIGURE 3 | Intranasal administration of extracellular vesicles from human induced pluripotent stem cell-derived neural stem cells (hiPSC-NSC-EVs) to late middle-aged mice reduced oxidative stress and normalized the mitochondrial respiratory chain gene expression. The bar charts A-J compare MDA (A, F), protein carbonyl (B, G), NRF-2 (C, H), SOD (D, I), and catalase (E, J) between aged-Veh and aged-EVs groups in males (A-E) and females (F-J). Heatmaps K and V compare the expression of multiple mitochondrial respiratory chain genes between aged-Veh and aged-EV groups in male (K) and female (V) mice. Bar charts L-U (male), and W-AF (female) show the relative expression of genes Ndufs6 (L, W), Ndufs7 (M, X), Sdha (N, Y), Sdhb (O, Z), Cyc1 (P, AA), Bcs1l (Q, AB), Cox7b (R, AC), Cox4i2 (S, AD), Slc25a1 (T, AE) and Atp6ap1 (U, AF) in aged-Veh and aged-EV groups. *, $p < 0.05$; **, $p < 0.01$; ***, $p < 0.001$; ****, $p < 0.0001$.

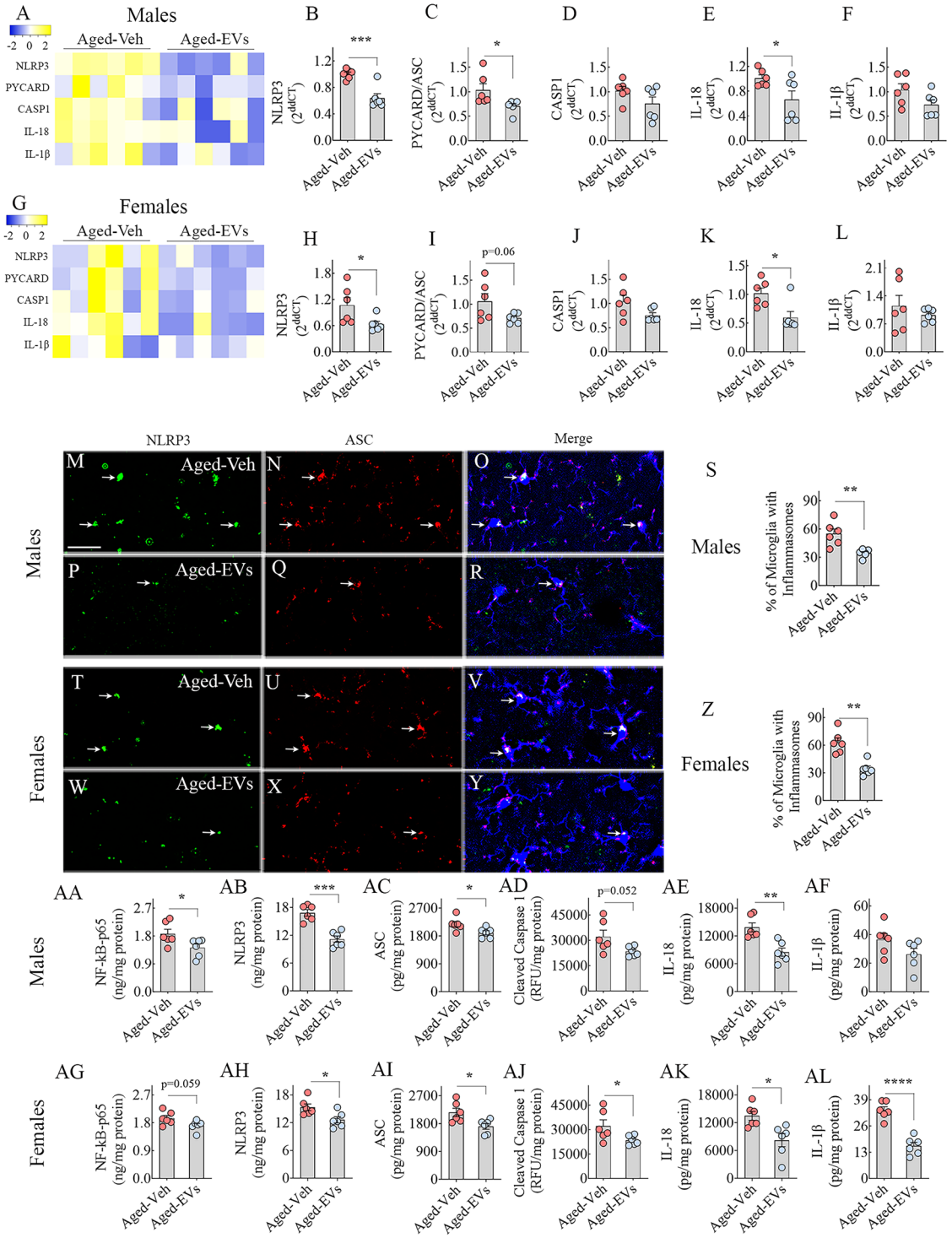

FIGURE 4 | Intranasal administration of extracellular vesicles from human induced pluripotent stem cell-derived neural stem cells (hiPSC-NSC-EVs) to late middle-aged mice inhibited NOD-, LRR-, and pyrin domain-containing protein 3 (NLRP3) and apoptosis-associated speck-like protein containing a CARD (ASC) inflammasome complex formation. Heatmaps A and G compare the expression of multiple NLRP3 inflammasome genes between aged-Veh and aged-EV groups in male (A) and female (G) mice. The bar charts B-F, H-L compare NLRP3 (B, H), PYCARD (C, I), CASP1 (D, J), IL-18 (E, K), and IL-1β (F, L) across aged-Veh and aged-EVs groups in males (B-F) and females (H-L). Figures M-R and T-Y illustrate examples of NLRP3 inflammasome complexes co-expressing NLRP3 (green) and ASC (red) in IBA-1+ microglia (blue) in the CA3 subfield of the hippocampus from male (M-R) and female (T-Y) mice belonging to aged-Veh (M-O, T-V) and aged-EVs (P-R, W-Y) groups. The bar charts S and Z compare the percentages of microglia with inflammasome complexes in males (S) and females (Z). The bar graphs AA-AL compare the concentrations of different proteins involved in the activation of NLRP3 inflammasomes, such as NF-kB p65 (AA, AG), NLRP3 (AB, AH), ASC (AC, AI), cleaved caspase-1 (AD, AJ), IL-18 (AE, AK), and IL-1β (AF, AL) between aged-Veh and aged-EVs groups of male (AA-AF) and female (AG-AL) mice. M-Y = 25 μm; *, $p < 0.05$; **, $p < 0.01$; ***, $p < 0.001$; ****, $p < 0.0001$.

EVs groups showed a similar trend with NLRP3, ASC, Cleaved Caspase-1, IL-18, and IL-1β showing significantly decreased concentrations than their counterparts in the aged-Veh group ($p < 0.05$–0.0001; Figure 4AH–AL). Two-way ANOVA analyses showed neither sex-dependent differences in Aged-Veh and aged-EVs groups nor interactions between sex and hiPSC-NSC-EVs treatment for all measured genes and a vast majority of the measured proteins linked to NLRP3 inflammasome activation ($p > 0.05$; Table S2). The exception is the concentration of NLRP3, which showed an interaction between sex and EVs treatment, although both males and females responded positively to EVs treatment ($p < 0.05$; Table S2). Thus, hiPSC-NSC-EV treatment in late middle-aged male and female mice significantly inhibited NLRP3 inflammasome activation in the aged hippocampus. Such effect was evident from reduced concentrations of (1) the transcription factor NF-kB-p65 that triggers the formation of NLRP3 inflammasome complexes, (2) proteins that facilitate their activation (NLRP3, ASC, and Cleaved Caspase-1), and (3) end products of NLRP3 inflammasome activation (IL-1β and IL-18).

3.8 | hiPSC-NSC-EVs Diminished the Activation of p38/MAPK Signalling in the Hippocampus

Since the end products of NLRP3 inflammasome activation (IL-1β and IL-18) and increased oxidative stress can mediate the downstream activation of p38/MAPK inflammatory signalling cascade (Figure 5A), the proficiency of hiPSC-NSC-EVs to reduce the concentrations of proteins involved in p38/MAPK signalling activation (Myd88, Ras, pMAPK, and AP-1) and some of the end products of p38/MAPK activation (TNF-α and IL-18) were measured (Figure 5B–M). In comparison to the aged-Veh group, both males and females in the aged-EVs group displayed decreased concentrations of all measured proteins, with Myd88, Ras, pMAPK, AP-1, and TNF-α showing a significant decline in both sexes ($p < 0.05$–0.001; Figure 5B–F, H–L). The concentration of IL-8 was significantly decreased in females ($p < 0.05$; Figure 5M) but showed only a trend in males ($p = 0.05$; Figure 5G). Two-way ANOVA analyses did not show sex-dependent differences in aged-Veh and aged-EVs groups for the concentrations of Myd88, Ras, AP-1, and IL-8 ($p > 0.05$; Table S2). The concentration of pMAPK showed sex-specific differences, with higher levels in females in the aged-EVs group ($p < 0.05$; Table S2). The concentration of TNF-α also showed sex-specific differences, with higher levels in the hippocampus of males within the aged-EVs group. However, post-hoc tests did not reveal significant differences (Table S2). Furthermore, no interaction was found between sex and hiPSC-NSC-EVs treatment for any of the proteins linked to p38/MAPK activation ($p > 0.05$; Table S2). Thus, hiPSC-NSC-EV treatment in late middle-aged male and female mice prevented p38/MAPK inflammatory signalling activation in the aged hippocampus.

3.9 | hiPSC-NSC-EVs Curtailed the Activation of cGAS-STING and the Downstream JAK-STAT Signalling and ISG Expression in the Hippocampus

As the cGAS–STING pathway and downstream JAK-STAT pathway (Figure 6A) is one of the drivers of aging-related inflammation in both peripheral organs and the brain (Gulen et al. 2023), the ability of hiPSC-NSC-EVs to reduce the concentrations of proteins involved in cGAS-STING signalling activation (p-cGAS, p-STING, p-TBK1, and p-IRF3) and one of its end products (IFN-α) was measured (Figure 6B–K). Compared with the aged-Veh group, both males and females in the aged-EVs group showed decreased concentrations of all measured proteins, with p-cGAS, p-STING, and p-IRF3 showing significant declines in both sexes ($p < 0.05$–0.01; Figure 6B, C, E, G-H, J). The concentration of p-TBK1 was significantly decreased in females ($p < 0.0001$, Figure 6I) but showed only a trend in males ($p = 0.058$; Figure 6D). The concentration of IFN-α was significantly decreased in males ($p < 0.001$, Figure 6F) but showed only a trend in females ($p = 0.0509$, Figure 6K). Two-way ANOVA analyses did not show sex-dependent differences in aged-Veh and aged-EVs groups for the concentrations of p-cGAS, p-STING, p-TBK1, and IFN-α ($p > 0.05$, Table S2). The concentration of p-IRF3 showed sex-specific differences, with higher levels in females in the aged-EVs group ($p < 0.05$, Table S2). Furthermore, no interaction was found between sex and hiPSC-NSC-EVs treatment for most of the proteins linked to cGAS-STING activation ($p > 0.05$; Table S2). The exception is the concentration of IFN-α, which showed an interaction between sex and EVs treatment, although both males and females responded positively to EVs treatment ($p < 0.05$; Table S2). Thus, hiPSC-NSC-EVs treatment in late middle age considerably diminished p38/MAPK inflammatory signalling activation in the hippocampus of both aged male and female mice.

Since increased release of IFN-α can lead to the activation of the downstream IFN-1 signalling through the JAK-STAT protein activation (Raftery and Stevenson 2017), the proficiency of hiPSC-NSC-EVs to reduce the concentrations of proteins involved in JAK-STAT signalling (p-JAK1, p-JAK2, p-STAT1, and p-STAT3) was measured (Figure 6L–S). Compared to the aged-Veh group, both males and females in the aged-EVs group displayed significantly decreased concentrations of p-JAK2 and p-STAT1 ($p < 0.05$, Figure 6M, N, Q, R). The concentration of p-JAK1 was significantly decreased in males ($p < 0.01$, Figure 6L) but showed only a decreased trend in females ($p = 0.056$, Figure 6P). The concentrations of p-STAT3 did not differ between aged-Veh and aged-EVs groups in both males and females ($p > 0.05$, Figure 6N, R). Two-way ANOVA analyses showed neither sex-dependent differences in aged-Veh and aged-EVs groups nor interactions between sex and hiPSC-NSC-EVs treatment for all measured proteins linked to JAK-STAT signalling ($p > 0.05$, Table S2). Thus, hiPSC-NSC-EVs treatment in late middle age considerably diminished JAK-STAT activation involved in IFN-1 signalling in the hippocampus of both aged male and female mice.

Next, we confirmed decreased expression of select ISGs in the hippocampus of both males and females in the aged-EVs groups compared to their counterparts in the aged-Veh groups (Figure 3A–R). In males receiving hiPSC-NSC-EVs, the expression of genes such as *Icam1, Cd47, Irf5, Irf7, IFNγ*, and *Tnf* was down-regulated ($p < 0.05$–0.01, Figure S3C–E, G–I). Whereas in females receiving hiPSC-NSC-EVs, the expression of *Icam1, Cd47*, and *Irf7* was reduced ($p < 0.05$–0.01, Figure S3L, M, P).

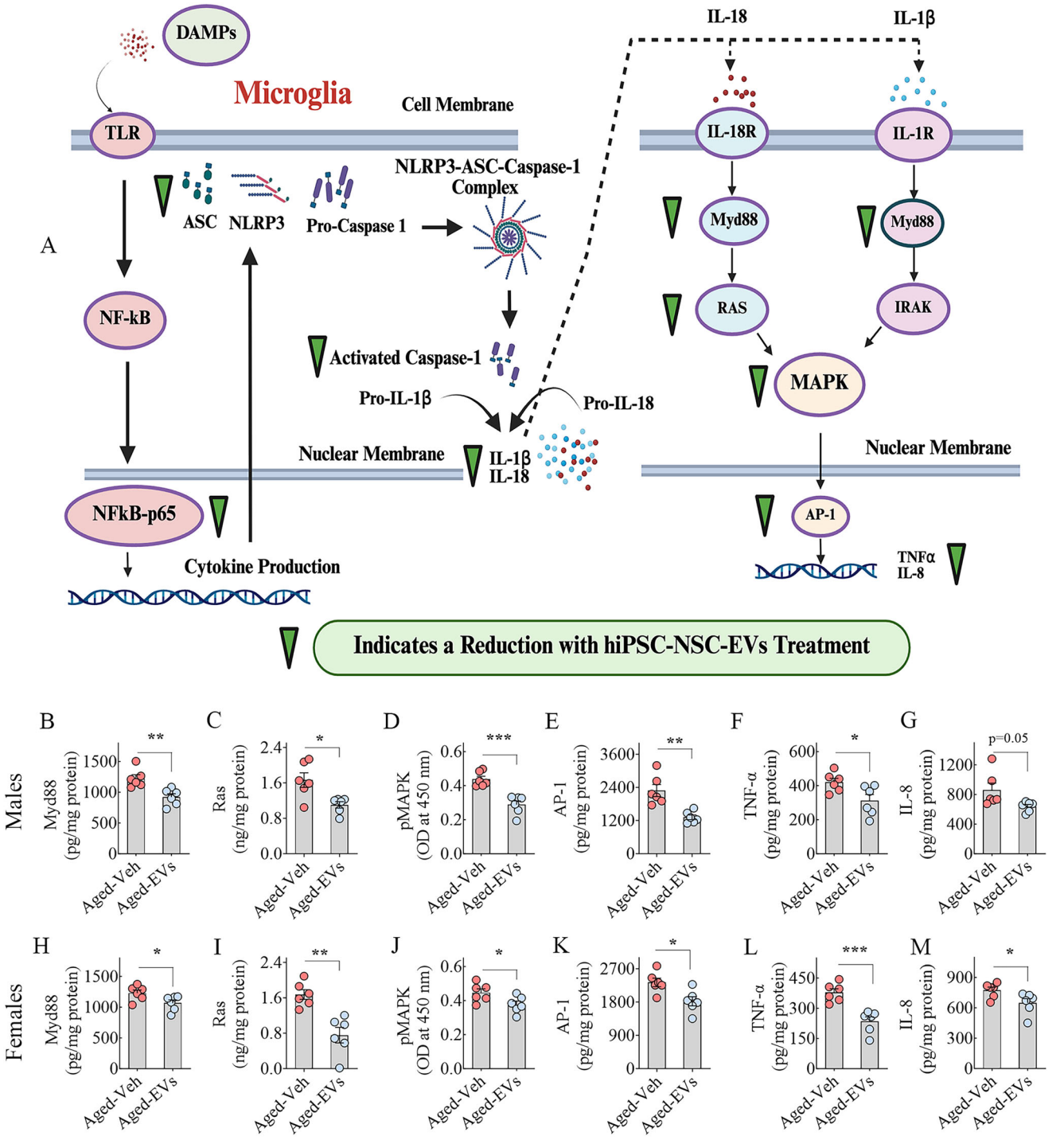

FIGURE 5 | Intranasal administration of extracellular vesicles from human induced pluripotent stem cell-derived neural stem cells (hiPSC-NSC-EVs) to late middle-aged mice inhibited p38/mitogen-activated protein kinase (p38/MAPK) signalling. Figure A is a cartoon depicting the various steps in NLRP3 inflammasome activation and how its end products (IL-18 and IL-1β) activate p38/MAPK signalling, leading to the increased production of proinflammatory cytokines in the aged brain. The downward-pointing green arrowheads depict various proteins that are reduced in concentration with hiPSC-NSC-EVs treatment. The bar charts in B-M compare the concentrations of p38MAPK signalling-related proteins between aged-Veh and aged-EVs groups in male and female mice. The proteins include Myd88 (B, H), Ras (C, I), pMAPK (D, J), transcription factor AP-1 (E, K), and end products such as TNF-α (F, L) and IL-8 (G, M) in male (B-G) and female (H-M) mice. *, $p < 0.05$; **, $p < 0.01$; ***, $p < 0.001$.

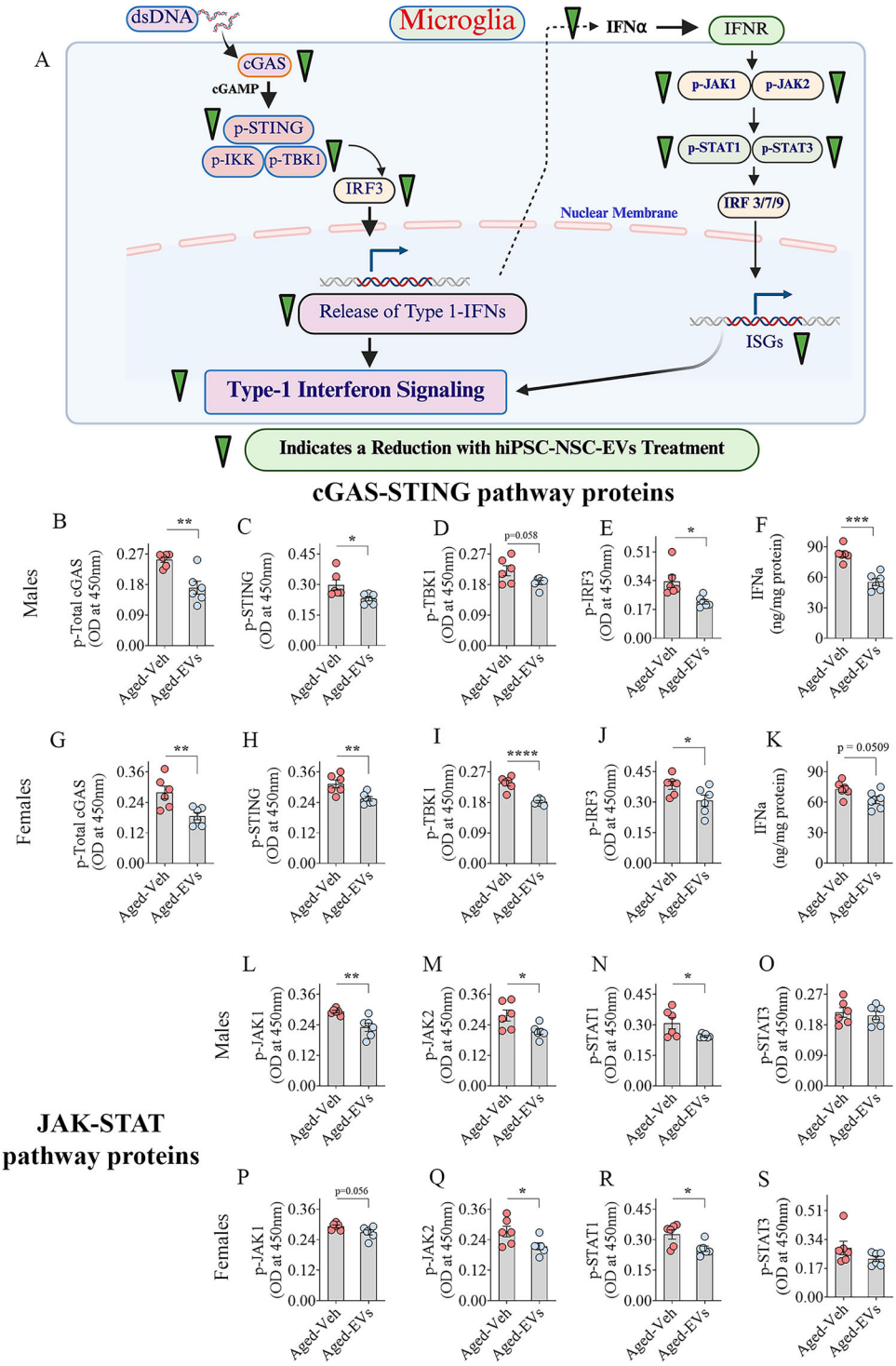

FIGURE 6 | Intranasal administration of extracellular vesicles from human induced pluripotent stem cell-derived neural stem cells (hiPSC-NSC-EVs) to late middle-aged mice inhibited cGAS-STING and JAK-STAT pathway activation. Figure A is a cartoon depicting the various steps in the activation of cGAS-STING-IFN-1 signalling in the aged brain. The downward-pointing green arrowheads depict various proteins in this signalling pathway that are reduced in concentration following hiPSC-NSC-EV treatment. The bar charts B-K compare the concentration of proteins linked to the cGAS-STING pathway, such as p-total cGAS (B, G), p-STING (C, H), p-TBK1 (D, I), p-IRF3 (E, J), and IFN-α (F, K) between Aged-Veh and Aged-EVs groups in male (B-F) and female (G-K) mice. The bar charts L-S compare the concentrations of proteins linked to the JAK-STAT pathway, including p-JAK1 (L, P), p-JAK2 (M, Q), p-STAT1 (N, R), and p-STAT3 (O, S) between Aged-Veh and Aged-EVs groups in male (L-O) and female (P-S) mice. *, $p < 0.05$; **, $p < 0.01$; ***, $p < 0.001$; ****, $p < 0.0001$.

3.10 | hiPSC-NSC-EVs Treatment in Late Middle-Age Led to Improved Cognitive Function in Old Age

We first examined whether anxiety levels varied between animals belonging to the Aged-Veh and Aged-EVs groups using data from an OFT (Figure 7A). Comparison of time spent in the central region of the open field and the frequency of entries into the central region revealed similar behaviour between aged-Veh and aged-EVs groups for both males and females ($p > 0.05$, Figure 7B–E). Thus, the results of cognitive and memory tests are not influenced by differences in anxiety levels between the aged-Veh and aged-EVs groups. We next investigated recognition and object-location memories using a NORT (Figure 7F) and an OLT (Figure 7N). In NORT, animals proficient in recognition memory prefer to explore the novel object (NO) over the familiar object (FO). In OLT, animals competent for object location memory prefer to explore the object in the novel place (OINP) over the object in the familiar place (OIFP). We initially confirmed that the male and female mice chosen for the study do display recognition and object-location memory impairments at the time point of hiPSC-NSC-EVs or Veh intervention. These results were obtained from separate cohorts of male and female mice to avoid the confounding effects of repeated behavioural testing on outcomes. These results are detailed in the Supplemental File (Figure S4).

We next examined cognitive and memory function in animals from the aged-Veh and aged-EVs groups between 19.5 and 20.5 months of age (i.e., commencing 1 month after the last Veh/EVs treatment). In NORT (Figure 7F–M), male and female mice in the aged-Veh group showed no preference to explore either the NO or the FO ($p > 0.05$; Figure 7H, K), whereas male and female mice in the aged-EVs group preferred to explore the NO for longer durations than the FO ($p < 0.001$; Figure 7I, L). Representative tracings of mouse movement from the aged-Veh and aged-EVs groups while exploring the FO and NO during trial-3 (T3) of an NORT are shown (Figure 7G). In OLT (Figure 7N–U), mice in the aged-Veh group showed a predilection for exploring the OIFP over the OINP ($p < 0.01$–0.001; Figure 7P, S), whereas mice in the aged-EVs group exhibited a preference to explore the OINP for longer durations than the OIFP ($p < 0.05$; Figure 7Q, T). Representative tracings of mouse movement from the aged-Veh and aged-EVs groups while exploring the OINP and OIFP in T3 of an OLT are shown (Figure 7O). Thus, male and female mice in the aged-Veh group displayed impairments in recognition and object location memory formation. In contrast, male and female mice in the aged-EVs groups exhibited proficiency in recognition and object location memory. Such a conclusion is also confirmed by significantly lower NO/OINP-DI values in male and female mice in the aged-Veh group compared to their counterparts in the aged-EVs group ($p < 0.05$–0.01; Figure 7J, M, R, U). The total object exploration times spent in trials 2 and 3 (T2 and T3) in NORT and OLT are presented in the supplemental file (Figure S5). Two-way ANOVA showed neither sex-dependent differences in aged-Veh and aged-EVs groups nor interactions between sex and hiPSC-NSC-EVs treatment for NO or OINP-DI values in both NORT and OLT ($p > 0.05$; Table S2).

3.11 | Depletion of miR-30e-3p Within hiPSC-NSC-EVs Diminished Their Ability to Inhibit NLRP3 Inflammasome Activation

By employing RAW-ASC cells that are transfected with the murine ASC gene, we investigated how hiPSC-NSC-EVs inhibit nigericin-induced NLRP3 activation (Figure 8A). For this, we first confirmed significantly reduced miR-30e-3p levels in EVs isolated from hiPSC-NSCs transfected with antagomirs targeting miR-30e-3p-5p. EVs from transfected hiPSC-NSCs displayed a ~79.61% decline in miR-30e-3p expression compared to EVs from naïve hiPSC-NSCs (Figure 8B). No such reduction was observed in EVs isolated from hiPSC-NSCs transfected with the scrambled miR-30e-3p-5p antagomir. A schematic representation of the experimental workflow is shown in Figure 8C. The culture media from RAW-ASC cells treated with nigericin showed increased levels of IL-1β and IL-18, compared to untreated cultures ($p < 0.0001$; Figure 8D–E). However, adding hiPSC-NSC-EVs after nigericin treatment markedly attenuated IL-1β and IL-18 levels compared with the nigericin-only group ($p < 0.001$–0.0001; Figure 8D–E). In contrast, adding hiPSC-NSC-EVs that are depleted of miR-30e-3p (knockdown EVs [KD-EVs]) did not reduce IL-1β and IL-18 levels compared to the nigericin alone group ($p > 0.05$, Figure 8D, E). Similar results were observed for the measurement of IL-1β and IL-18 in the cell lysates of these cultures (Figure 8F, G). Collectively, these findings suggested that miR-30e-3p is the primary active component in hiPSC-NSC-EVs that inhibit NLRP3 inflammasome activation.

3.12 | Depletion of miR-181a-5p Within hiPSC-NSC-EVs Diminished Their Ability to Inhibit STING Activation

By employing RAW-Lucia-ISG cells, we investigated how hiPSC-NSC-EVs inhibit 2',3' cGAMP -induced STING activation (Figure 8H). For this, we first confirmed significantly reduced miR-181a-5p levels in EVs isolated from hiPSC-NSCs transfected with antagomirs targeting miR-181a-5p. EVs from transfected hiPSC-NSCs displayed a ~72.81% decline in miR-181a-5p expression compared to EVs from naïve hiPSC-NSCs (Figure 8I). No such reduction was observed in EVs isolated from hiPSC-NSCs transfected with the scrambled miR-181a-5p antagomir. A schematic representation of the experimental steps is shown in Figure 8J. The culture media of RAW-Lucia-ISG cells treated with 2',3' cGAMP showed increased Lucia luciferase activity compared to untreated cultures ($p < 0.0001$, Figure 8K). However, adding hiPSC-NSC-EVs after 2',3' cGAMP treatment markedly reduced Lucia luciferase activity compared with the 2',3' cGAMP-only group ($p < 0.05$; Figure 8K). In contrast, adding hiPSC-NSC-EVs that are depleted of miR-181a-5p (KD-EVs) did not reduce Lucia luciferase activity compared to the 2',3' cGAMP-only group ($p > 0.05$, Figure 8K). We also measured IFN-α levels in lysates from RAW-Lucia-ISG cells across different groups. A significant increase in IFN-α concentration was observed in RAW-Lucia-ISG cells treated with 2',3' cGAMP alone compared to untreated cultures ($p < 0.0001$, Figure 8L). However, RAW-Lucia-ISG cells treated with 2',3' cGAMP and naïve hiPSC-NSC-EVs displayed a

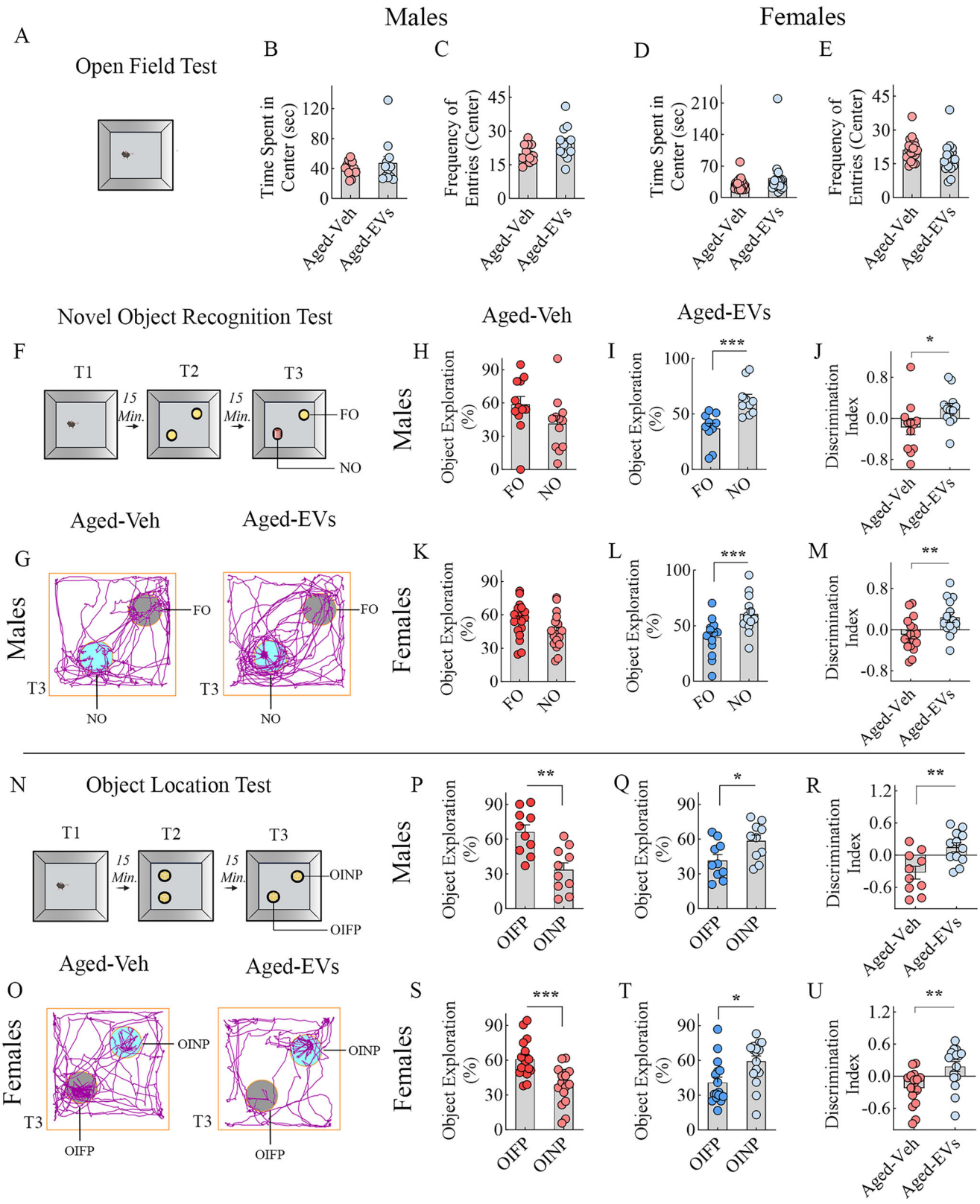

FIGURE 7 | Intranasal administration of extracellular vesicles from human induced pluripotent stem cell-derived neural stem cells (hiPSC-NSC-EVs) to late middle-aged mice improved cognitive dysfunction. Cartoon A depicts the open field test (OFT). Bar chart B-E compares the time spent in the centre (B, D) and frequency of entries to the centre (C, E) in males (B-C) and females (D-E) between AD-Veh and AD-EVs groups. Cartoon F depicts different trials (T1-T3) in a novel object recognition test (NORT). Representative tracings in G illustrate the exploration of objects by male mice from the Aged-Veh and Aged-EVs groups in T3. The bar charts in H-I and K-L compare percentages of object exploration times spent with the familiar object (FO) vis-à-vis the novel object (NO) between Aged-Veh (H, K) and Aged-EV groups (I, L) for males (H-I) and females (K-L). The bar charts J and M compare the NO discrimination index values between Aged-Veh and Aged-EVs groups in males (J) and females (M). Cartoon N depicts different trials (T1-T3) in an object location test (OLT). Representative tracings in O illustrate the exploration of objects by female mice from aged-Veh

reduced concentration of IFN-α (p <0.01, Figure 8L). In contrast, RAW-Lucia-ISG cells treated with 2',3' cGAMP and hiPSC -NSC-EVs that are depleted of miR-181a-5p did not show reduced IFN-α (p > 0.05, Figure 8L). Overall, these findings suggested that miR-181a-5p is the primary active component in hiPSC-NSC-EVs that inhibit STING activation.

3.13 | Interaction With hiPSC-NSC-EVS Triggered Widespread Transcriptomic Changes in Aged Microglia

From sc-RNA-seq data, we first examined the t-SNE plots, which did not show clear separation between aged-Veh and aged-EVs groups (Figure S6). Analysis of DEGs (p < 0.01) revealed upregulation of 896 genes and downregulation of 2025 genes in the aged-EVs group vis-à-vis the aged-Veh group (Figure 9A). The KEGG enrichment analysis (KEGG mouse 2019) of DEGs with p < 0.01 between the aged-Veh and aged-EVs groups determined that these genes were mapped in 71 pathways, including Alzheimer's disease, Oxidative phosphorylation, Toll-like receptor (TLR) signalling pathway, MAPK signalling pathway, TNF signalling pathway, C-type lectin receptor signalling pathway, mechanistic target of rapamycin (mTOR) signalling pathway, ForkHead box (FoxO) signalling pathway, Notch signalling pathway, Ras-related protein 1 (Rap1) signalling pathway, and Ubiquitin-mediated proteolysis (Figure 9B). Analysis of DEGs mapped in these pathways between the aged-Veh and aged-EVs groups revealed upregulation of numerous genes in AD, in which the majority of DEGs were associated with mitochondrial function. Interestingly, all DEGs associated with oxidative phosphorylation were also significantly upregulated in the aged-EVs group compared to the aged-Veh group, implying enhanced mitochondrial activity following EVs treatment in late middle-aged mice (Figure 9C, D). Furthermore, hiPSC-NSC-EVs treatment in aged mice modulated the transcriptome of multiple neuroinflammatory pathways in microglia, where many DEGs in the TLR signalling pathway, MAPK signalling pathway, TNF signalling pathway, and the C-type lectin receptor signalling pathway were significantly downregulated in the aged-EVs group, implying reduced neuroinflammatory signalling with hiPSC-NSC-EVs treatment (Figure 10A–D). Furthermore, multiple DEGs in longevity-related pathways, including the mTOR signalling pathway, FoxO signalling pathway, and Notch signalling pathways, were significantly downregulated (p < 0.01) in the microglia of the aged-EVs group (Figure 10E–G). Additionally, multiple DEGs in pathways such as Rap1 signalling and ubiquitin-mediated proteolysis were significantly downregulated following hiPSC-NSC-EVs treatment in late middle-aged mice (Figure S7A, B).

We also performed microglial cluster extraction based on the DEGs between the clusters (Tables 3–6), which yielded five different clusters (Figure 11A). The KEGG pathway analysis of DEGs in clusters 1–5 revealed involvement in multiple signalling pathways, including those related to neuroinflammation (Figures S8 and S9). Among these, DEGs in cluster 1 are enriched for the TLR signalling pathway. The expression of genes such as *Pik3cd* and *Map3k8* was significantly reduced by hiPSC-NSC-EVs treatment in this microglial cluster (Figure 11B). The DEGs of cluster 2 are involved in IL-17 signalling and cholesterol metabolism. The expression of genes involved in IL-17 signalling, such as *Lcn2, S100a8*, and *S100a9*, was significantly reduced in microglia from the Aged-EVs group compared to microglia from the Aged-Veh group. Similarly, the expression of genes such as *Ldlr* and *Lpl*, involved in cholesterol metabolism, was significantly increased in microglia from the Aged-EVs group (Figure 11C, D). The DEGs of cluster 4 are found to be involved in IL-17 signalling, nucleotide-binding oligomerization domain (NOD)-like receptor signalling, and Rap1 signalling (Figure 11E–G). In IL-17 signalling, the expression of genes such as *Lcn2, S100a8*, and *S100a9* was significantly decreased in microglia from the Aged-EVs group (Figure 11E). In the NOD-like receptor pathway, the expression of genes such as *Gbp2, Oas1a*, and *Oas1g* was increased, and *Camp* was decreased in microglia from the Aged-EVs group (Figure 11F). In the Rap1 signalling, *Adcy8* and *Thbs1* genes were downregulated, and *Flt1* and *Igf1* were upregulated in microglia from the Aged-EVs group (Figure 11G). Thus, cluster analysis also revealed modulation of proinflammatory and cholesterol metabolism signalling pathways in microglia from mice receiving hiPSC-NSC-EVs.

Next, we performed GeneWalk analysis, yielding a scatterplot based on gene connections and fractions of relevant GO terms (Figure 11H). The most significant genes with >100 gene connections and the highest fractions of relevant GO terms (1:00) were identified. Among these, *Nrf1*, *Sec24C*, and *Fos* was downregulated in microglia from the Aged-EVs group compared to microglia from the Aged-Veh group (Figure 11H). These genes play significant roles in promoting microglia-mediated inflammatory pathways; hence, reduced expression of these genes is consistent with the diminished neuroinflammaging observed in the Aged-EVs group. In addition, the expression of the *Nfe2l1* gene was upregulated in the Aged-EVs group, which is significant because Nfe2l1 is known to maintain redox balance by stimulating antioxidant genes and maintaining mitochondrial homeostasis. Thus, GeneWalk analysis also confirmed a diminished proinflammatory transcriptome in microglia following treatment with hiPSC-NSC-EVs.

4 | Discussion

The results provide the first evidence that IN administration of hiPSC-NSC-EVs in late middle-aged mice can diminish the proinflammatory transcriptome within microglia in the aged brain. Such a change correlated with reductions in oxidative stress, mitochondrial dysfunction, and neuroinflammaging, and

and aged-EVs groups in T3. The bar charts in P-Q and S-T compare percentages of object exploration times spent with the object in the familiar place (OIFP) vis-à-vis the object in the novel place (OINP) between aged-Veh (P, S) and aged-EV groups (Q, T) in males (P-Q) and Females (S-T). The bar charts R and U compare the OINP discrimination index values between Aged-Veh and Aged-EVs groups in males (R) and females (U). *, p < 0.05; **, p < 0.01; ***, p < 0.001.

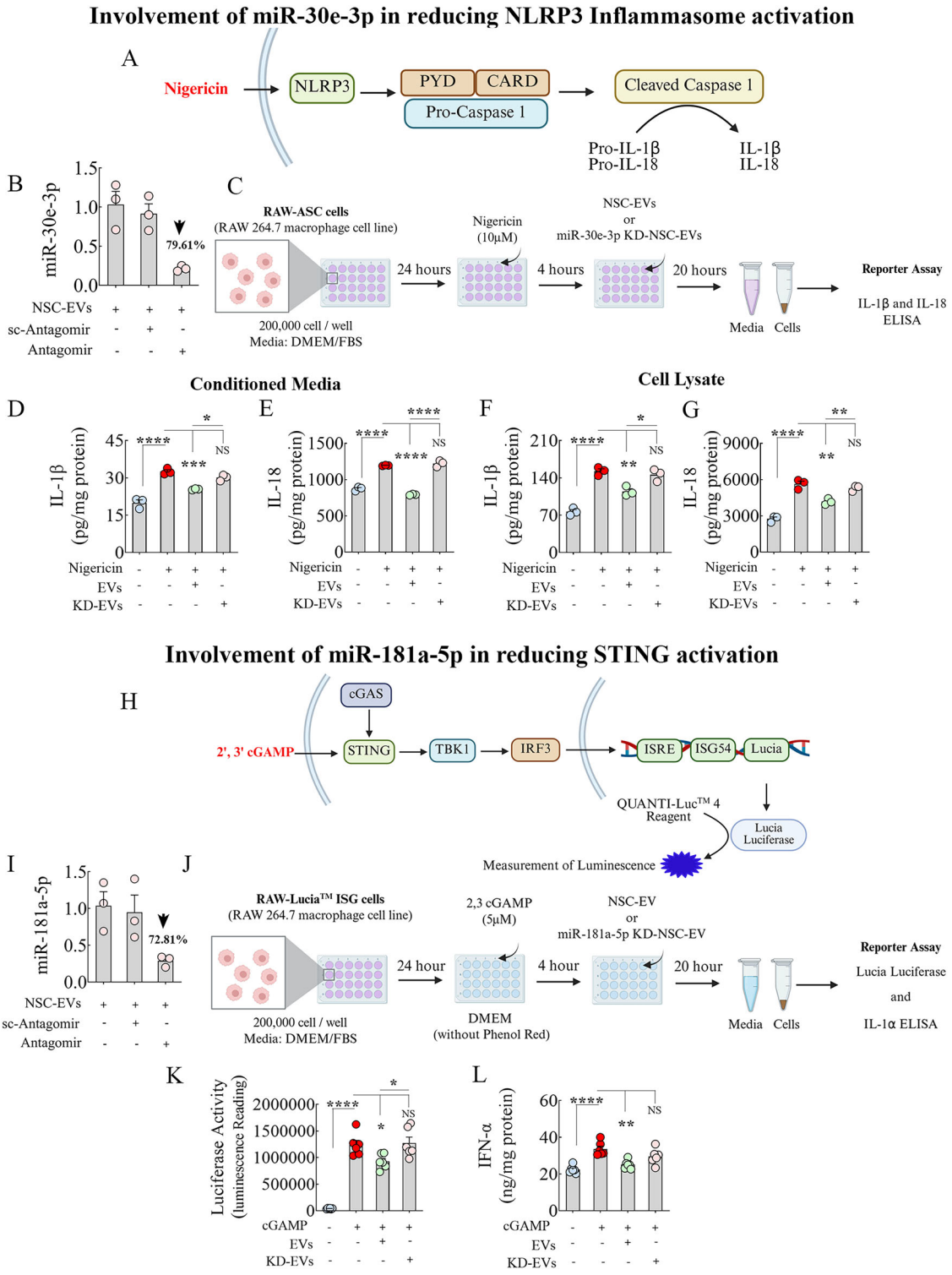

FIGURE 8 | Depletion of miR-30e-3p in extracellular vesicles from human induced pluripotent stem cell-derived neural stem cells (hiPSC-NSC-EVs) diminished their ability to inhibit NLRP3 Inflammasome activation, and depletion of miR-181a-5p within hiPSC-NSC-EVs reduced their ability to inhibit STING activation. Cartoon A depicts the sequential changes following NLRP3 stimulation by Nigericin in RAW-ASC cells, culminating in the release of IL-1β and IL-18. Bar chart B compares the levels of miR-30e-3p in EVs derived from naive, miR-30e-3p antagomir-treated, or miR-30e-3p scrambled-antagomir-treated hiPSC-NSCs. Cartoon C illustrates the research design used to test the effects of naive hiPSC-NSC-EVs, hiPSC-NSC-EVs depleted of miR-30e-3p (KD-EVs), on RAW-ASC cells following nigericin stimulation. Bar charts D-G compare the concentrations of IL-1β (D, F) and IL-18 (E, G) in conditioned media (D-E), and cell lysates (F-G) of RAW-ASC cell cultures between various treatment groups. Cartoon H depicts the sequential changes following STING activation by 2', 3' cGAMP stimulation in RAW-Lucia-ISG cells, culminating in increased luciferase activity, implying the activation of the TBK-1-IRF3 axis and the production of type 1 IFNs. Bar chart I compares the levels of miR-181a-5p in EVs derived from naive, miR-181a-5p antagomir-treated, or miR-181a-5p scrambled-treated hiPSC-NSCs. Cartoon J illustrates the research design used to test the effects of naive hiPSC-NSC-EVs, hiPSC-NSC-EVs depleted of miR-181a-5p (KD-EVs), on RAW-Lucia-ISG cells following 2', 3'

improved cognitive and memory function observed in aged mice receiving hiPSC-NSC-EVs. Furthermore, the antiinflammatory effects of hiPSC-NSC-EVs were associated with decreased activation of key signalling pathways, including NLRP3, p38/MAPK, cGAS-STING, JAK-STAT, and IFN-1 in the aged hippocampus.

4.1 | Effect of hiPSC-NSC-EVs Treatment on Oxidative Stress in the Aged Hippocampus

Increased oxidative stress is a key alteration in brain aging (Ionescu-Tucker and Cotman 2021), characterized by elevated ROS levels that lead to mitochondrial dysfunction and synaptic damage in neurons (Grimm and Eckert 2017). Such changes contribute to cognitive impairments and the progression of neurodegenerative diseases like AD. Mitochondria generate most free radicals during energy production, and the accumulation of ROS disrupts redox homeostasis, leading to genomic instability and the transcription of many proinflammatory genes (Ionescu-Tucker and Cotman 2021; Islam 2017). Moreover, increased ROS can damage mitochondrial DNA, further impairing neuronal function (Ionescu-Tucker and Cotman 2021; Islam 2017; Lu et al. 2004). Therefore, strategies to reduce oxidative stress and protect the mitochondrial electron transport chain are crucial for preventing cognitive decline in old age. In this context, the current study shows that hiPSC-NSC-EVs treatment effectively reduces oxidative stress in the aged hippocampus of late-middle-aged male and female mice. These were evidenced by lower levels of MDA and PCs, which indicate reduced lipid peroxidation and protein oxidation, alongside increased NRF-2 and SOD levels, key components of antioxidant defence. Additionally, gene expression for many mitochondrial respiratory chain proteins was normalized in treated mice. The neuroprotective protein hemopexin, enriched in the hiPSC-NSC-EVs (Upadhya et al. 2020), may contribute to this protective effect against oxidative stress, given its role in safeguarding neurons from heme and ROS (Hahl et al. 2013). Additionally, diminished proinflammatory microglial transcriptome induced by hiPSC-NSC-EVs has likely contributed to reduced oxidative stress, as persistent neuroinflammation can elevate oxidative stress in the neuronal microenvironment. Such changes in microglia in the hippocampus of mice receiving hiPSC-NSC-EVs were evident from lower expression of numerous proinflammatory genes, higher expression of many genes that enhance oxidative phosphorylation, and reduced activation of several microglia-mediated proinflammatory signalling pathways.

4.2 | Impact of hiPSC-NSC-EVs on Neuroinflammatory Signalling Cascades in the Aged Hippocampus

Age-related neuroinflammation, or neuroinflammaging, is a significant aspect of brain aging (Britton et al. 2022; Mosher and Wyss-Coray 2014). In C57BL/6 mice, the incidence of neuroinflammation increases with age, accompanied by notable changes in microglia, including increased proliferation, reactivity, and motility, as well as altered gene expression (Long et al. 1998; Harry 2013; Hefendehl et al. 2014). Aging microglia express proinflammatory markers such as IL-1β, TNF-α, and IL-6, resulting in a chronic inflammatory environment detrimental to neuronal function (Wolf and Boddeke 2017; Yu et al. 2002). Key neuroinflammatory pathways, particularly the NLRP3 inflammasome, are activated in this context (Fu et al. 2020; He et al. 2021). Triggered by DAMPs like ROS and cellular debris, the NLRP3-ASC inflammasome complex activates caspase-1, leading to the maturation and increased release of IL-1β and IL-18 (Ayyubova and Madhu 2025). These changes initiate downstream signalling primarily through the p38/MAPK pathway, leading to the sustained release of proinflammatory cytokines and perpetuating chronic neuroinflammation (Kodali et al. 2023; Madhu et al. 2024). Activation of the cGAS-STING-IFN-1 signalling is another pathway that plays a key role in neuroinflammaging (Gulen et al. 2023). Triggered by sensing dsDNA or mtDNA, this pathway leads to increased production of type 1-IFN, which is crucial for antiviral defence and immune regulation (Gulen et al. 2023; Madhu et al. 2024; Jimenez-Loygorri et al. 2024). These interferons then signal through the JAK-STAT pathway to promote the transcription of interferon-stimulated genes (ISGs), thereby driving neuroinflammation and altered immune responses (Gulen et al. 2023; Paul et al. 2021; Baruch et al. 2014).

Thus, moderate chronic neuroinflammation, driven by NLRP3-p38/MAPK and cGAS-STING-IFN-1 signalling in the brain, significantly contributes to cognitive decline with aging. Targeting these pathways may help maintain cognitive function in old age. The current study found that hiPSC-NSC-EVs treatment in late-middle-aged mice reduced chronic neuroinflammation in the hippocampus, as evidenced by decreased proinflammatory transcriptomic signatures in microglia and a less proinflammatory microenvironment. First, treatment reduced microglial cluster formation and lowered the percentage of microglia with NLRP3 inflammasome complexes. Second, significant reductions in key proteins that activate the NLRP3 inflammasome and the p38/MAPK pathway were observed, including NLRP3, ASC, cleaved Caspase-1, pMAPK, and AP-1. Third, levels of proteins in the cGAS-STING-IFN-1 and JAK-STAT signalling cascades, such as p-cGAS, p-STING, p-IRF3, IFN-α, p-JAK1/2, and p-STAT1, as well as in ISG expression, were notably decreased. These changes were consistent in both male and female mice treated with hiPSC-NSC-EVs compared with vehicle-treated controls. Thus, hiPSC-NSC-EVs can slow chronic neuroinflammation in the aged brain by modulating the microglial proinflammatory transcriptome and inflammatory signalling cascades.

4.3 | Direct Effects of hiPSC-NSC-EVs on Microglia in the Aged Hippocampus

Our earlier studies have shown that hiPSC-NSC-EVs can significantly lower IL-6 release from LPS-stimulated macrophages and IL-1β and TNF-α release from LPS-stimulated hiPSC-derived iMicroglia (Upadhya et al. 2020, 2022). Additionally, in neu-

cGAMP stimulation. Bar chart K compares luciferase activity in conditioned media of RAW-Lucia-ISG cells between various treatment groups. Bar chart L compares IFN-α concentration in cell lysates of RAW-Lucia-ISG cells between various treatment groups.

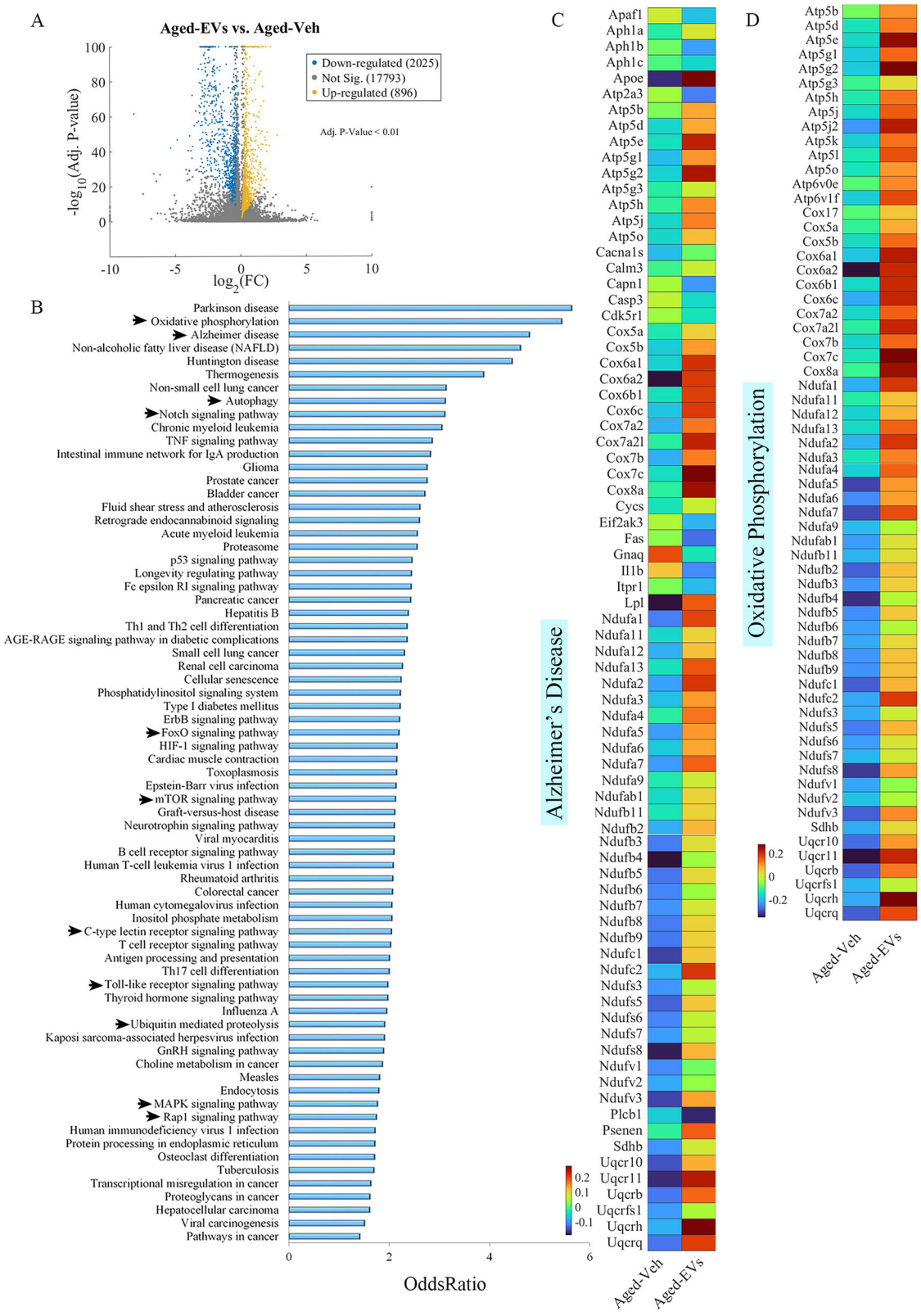

FIGURE 9 | **Intranasal administration of extracellular vesicles from human induced pluripotent stem cell-derived neural stem cells (hiPSC-NSC-EVs) induced widespread transcriptomic changes in microglia of late middle-aged male mice.** The volcano plot in A displays differentially expressed genes (DEGs) that are significantly downregulated (blue) or upregulated (yellow) in the mouse from the Aged-EVs group compared to the mouse from the Aged-Veh group. Figure B illustrates the involvement of differentially expressed genes (DEGs) in the most significant pathways identified from KEGG enrichment pathway analysis. Heatmaps C and D compare the expression of various genes involved in pathways linked to Alzheimer's disease (C) and oxidative phosphorylation (D) between the Aged-Veh and Aged-EVs groups.

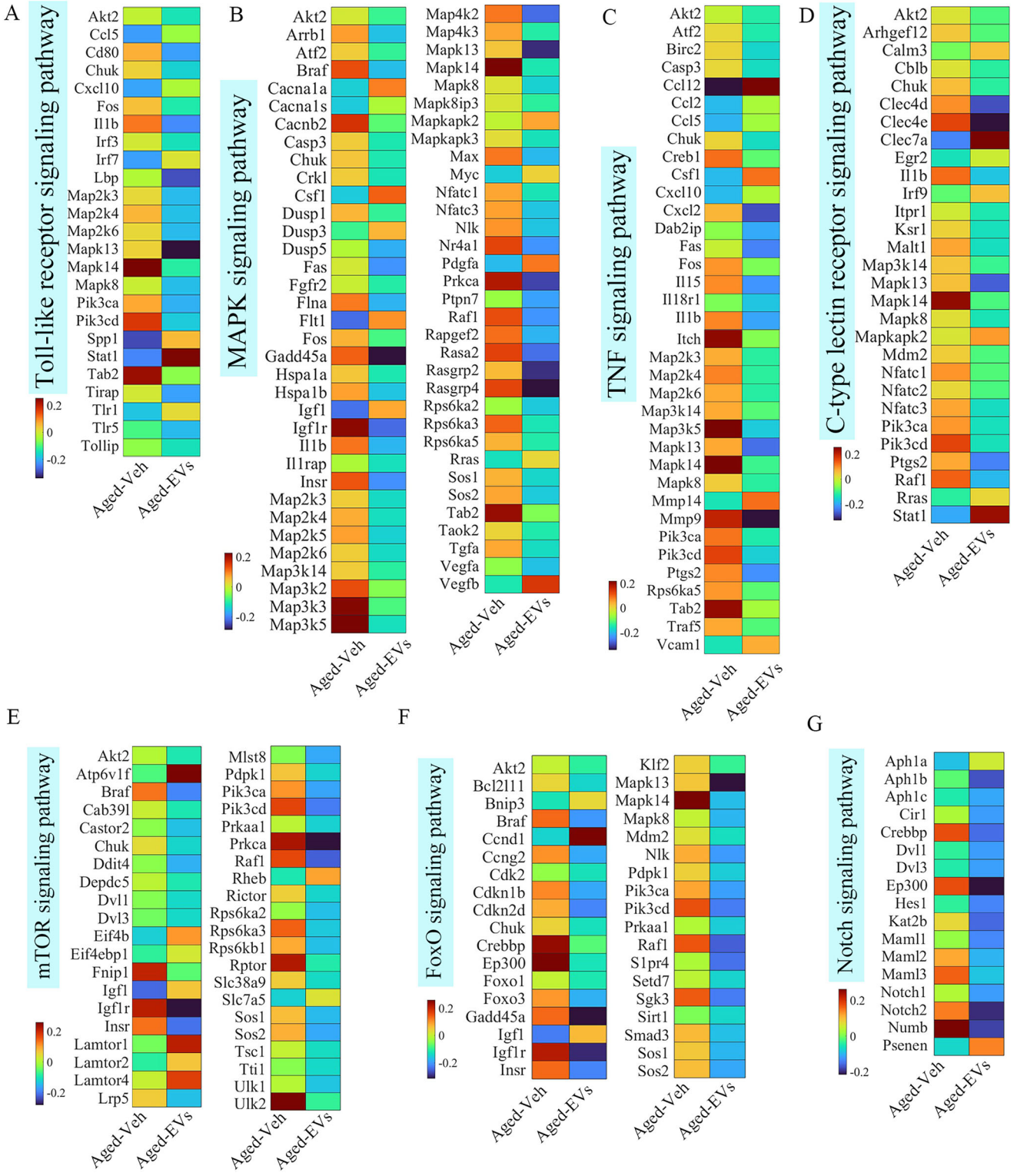

FIGURE 10 | **Intranasal administration of extracellular vesicles from human induced pluripotent stem cell-derived neural stem cells (hiPSC-NSC-EVs) reduced the expression of numerous genes implicated in many proinflammatory signalling pathways.** Heatmaps in A-G compare the expression of genes involved in the Toll-like receptor (A), mitogen-activated protein kinase (MAPK) (B), tumour necrosis factor (TNF) (C), C-type lectin receptor (D), mechanistic target of rapamycin (mTOR) (E), ForkHead box (FoxO) (F), and Notch (G) signalling pathways between Aged-Veh and Aged-EVs groups.

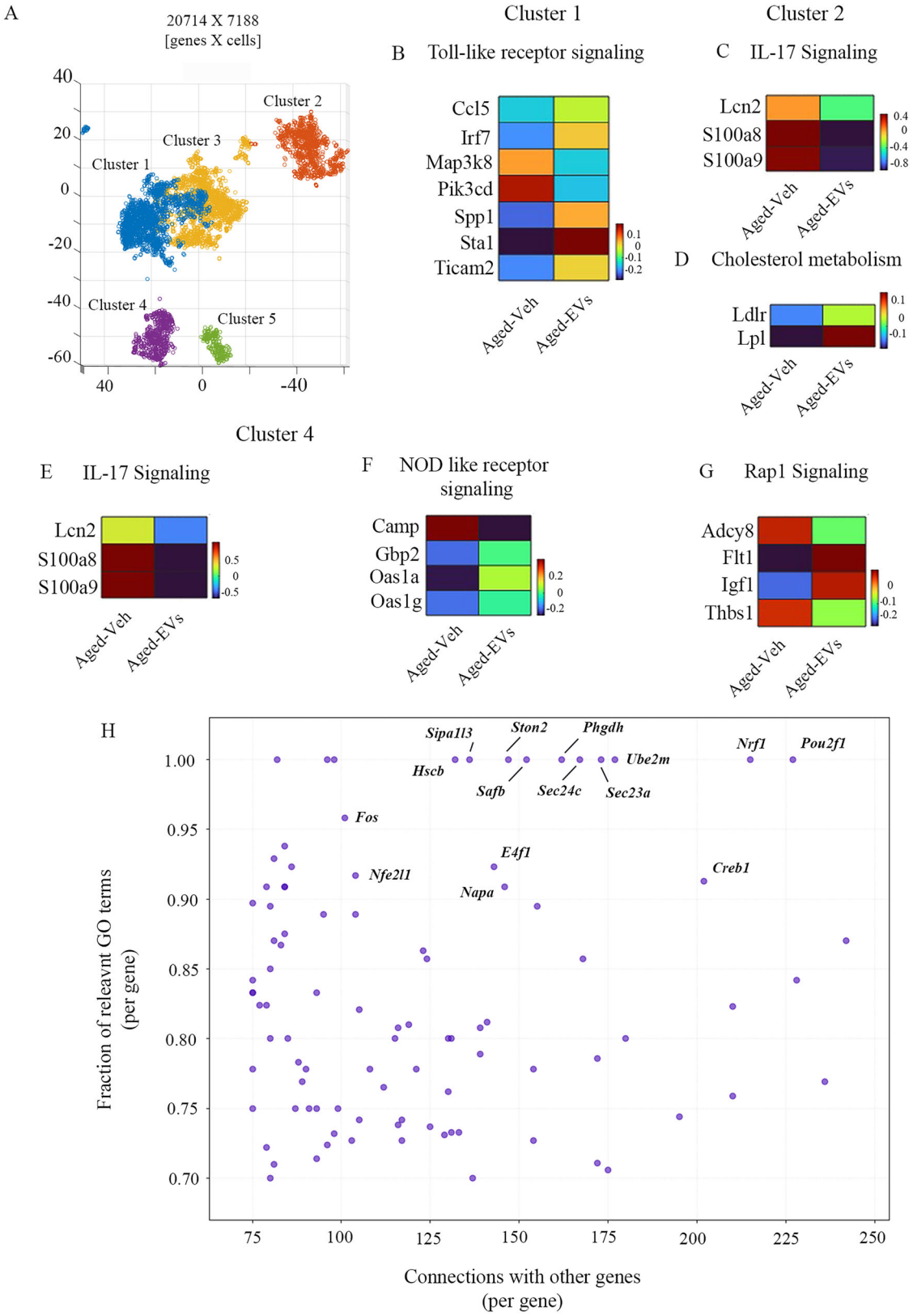

FIGURE 11 | KEGG pathway analysis of DEGs in clusters 1-5 and GeneWalk Analysis. Figure A shows a t-SNE plot showing five distinct microglia clusters from late middle-aged male mice treated with extracellular vesicles from human induced pluripotent stem cell-derived neural stem cells (hiPSC-NSC-EVs) or vehicle. Heat maps in B-H compare the expression of genes identified in the most significant pathways identified from KEGG enrichment pathway analysis. These include the Toll-like receptor signalling pathway (B) from cluster 1; IL-17 (C) and cholesterol metabolism (D) signalling pathways from cluster 2; and IL-17 (E), nucleotide-binding oligomerization domain (NOD)-like receptor (F), and Ras-related protein 1 (Rap1) (G) signalling pathways from cluster 4. The scatter plot in H shows regulatory genes, identified through GeneWalk analysis, with various fractions of relevant gene ontology (GO) terms and variable connections to other genes.

roinflammatory conditions, such as in rodent models of status epilepticus or LPS-induced neuroinflammation, hiPSC-NSC-EVs markedly decreased microglia-mediated neuroinflammation (Upadhya et al. 2020; Ayyubova et al. 2023). Our recent study also indicated that hiPSC-NSC-EVs can modulate disease-associated microglia in 5xFAD mice without affecting their phagocytic activity (Madhu et al. 2024). More importantly, in the current study, scRNA-seq analysis of microglia 7 days after hiPSC-NSC-EVs administration showed that these EVs can alter the proinflammatory microglial transcriptome. hiPSC-NSC-EVs treatment enhanced the expression of genes related to AD, mitochondrial function, and cholesterol metabolism while reducing the expression of genes linked to neuroinflammatory pathways. Key pathways affected include AD and oxidative phosphorylation, with upregulation of genes crucial for mitochondrial respiratory chain integrity, which is beneficial as reduced expression of these genes is associated with mitochondrial dysfunction in aging and AD (Olesen et al. 2020; Baik et al. 2019; Miao et al. 2023). Increased expression of genes (*Ldlr and Lpl1*) related to cholesterol metabolism is also advantageous, as deficiency of these genes promotes microglial proliferation, activation, and lipid droplet accumulation (Rodrigues et al. 2024; Loving et al. 2021). The diminished proinflammatory pathways in microglia mediated by hiPSC-NSC-EVs include TLR, NOD, MAPK, TNF, C-type lectin receptor, and IL-17 signalling. Such effects have immense value, as aging, AD, or neurodegenerative diseases are associated with increased expression of genes promoting TLR (Edler et al. 2021), NOD (Terzioglu and TL 2023), MAPK (Viorel et al. 2024), TNF (Bhaskar et al. 2014; Valiukas et al. 2025), and C-type lectin receptor (Nascimento et al. 2025) signalling pathways. Moreover, decreased expression of genes linked to NOD-signalling, such as *Pik3cd* and *Map3k8*, has therapeutic value, as they promote microglial activation (Hawkins and Stephens 2015; Wang et al. 2023). Also, decreased expression of genes (*Lcn2, S100a9,* and *S100a8*) involved in IL-17 signalling is important, as these genes are implicated in the induction of a proinflammatory signature in microglia (Zhang et al. 2025; Pampuscenko et al. 2025; Gruel et al. 2024).

Furthermore, the expression of many genes associated with mTOR, FoxO, Notch, Rap1 signalling, and the ubiquitin-mediated proteolysis pathway was significantly downregulated in mice treated with hiPSC-NSC-EVs. These changes also carry significant implications for neuroinflammaging. For instance, heightened mTOR signalling in microglia contributes to a primed inflammatory state in the aged brain (Keane et al. 2021). On the other hand, increased activity of FoxO transcription factors, such as FoxO3, can lead to greater microglial activation (Shang et al. 2009a, 2009b). Conversely, elevated Notch signalling can further amplify microglial activation in neuroinflammatory conditions (Wu et al. 2018), and enhanced Rap1 signalling is known to drive neuroinflammation (Wei et al. 2025). Interestingly, the reduced expression of genes related to the ubiquitin-mediated proteolysis pathway is unexpected, given its crucial role in clearing ubiquitylated protein aggregates (Ndoja et al. 2020). This downregulation may reflect a compensatory mechanism or the brain's effort to restore balance in a microenvironment characterized by lower oxidative stress and reduced neuroinflammation, mediated by hiPSC-NSC-EVs treatment. Additionally, GeneWalk analysis revealed four regulatory genes with over 100 connections and GO term scores exceeding 0.95, all relevant to microglial function. These include *Nrf1, Sec24c, Fos*, and *Nfe2l1*. Notably, the expression of *Nrf1, Sec24c*, and Fos was downregulated in aged mice receiving hiPSC-NSC-EVs, suggesting an advantage. First, decreased *Nrf1* expression in microglia can reduce the production of proinflammatory cytokines TNF-α and IL-1β (Wang et al. 2022). Second, decreased *Sec24c* expression can reduce STING activation, as Sec24c is required for STING oligomerization (Seok et al. 2023). Third, decreased *Fos* expression can reduce neuroinflammatory response in the hippocampus (Nomaru et al. 2014). Furthermore, *Nfe2l1* expression was upregulated, which is significant because it helps maintain redox balance by stimulating antioxidant genes and supporting mitochondrial homeostasis (Liu et al. 2023 Sep). Thus, hiPSC-NSC-EVs treatment in late middle-aged mice promoted robust antiinflammatory effects on microglia.

4.4 | Mechanisms by Which hiPSC-NSC-EVs Alleviated Neuroinflammation in the Aged Hippocampus

The miRNA and protein composition of hiPSC-NSC-EVs employed in this study provides insights into their potential antiinflammatory mechanisms in the aged hippocampus. Our previous studies have identified miRNAs, such as miR-21-5p and miR-103a, and proteins, such as pentraxin-3 (PTX3), hemopexin, and galectin-3 binding protein (Gal3BP), in hiPSC-NSC-EVs that can promote antiinflammatory effects (Upadhya et al. 2020, 2022). For example, miR-21-5p can enhance antiinflammatory activity by modulating NF-κB signalling, increasing IL-10 levels, and inhibiting TNF-α release (Ge et al. 2016; Sheedy 2015; Slota and Booth 2019; Barnett et al. 2016). Whereas PTX3 can stimulate beneficial A2 astrocytes and help maintain the blood-brain barrier (Shindo et al. 2016; Rajkovic et al. 2019; Zhou et al. 2020). Additionally, miR-103a, hemopexin, and Gal3BP can substantially reduce neuroinflammation and promote the transition of microglia from a proinflammatory to an antiinflammatory state (Blurton-Jones et al. 2009; Yang et al. 2018; Han et al. 2018; Seki et al. 2020). More importantly, cell culture experiments with engineered RAW-ASC and RAW-Lucia-ISG cells in this study provide evidence that miR-30e-3p and miR-181a-5p are involved in the inhibition of the NLRP3 inflammasome and cGAS-STING pathway, respectively, by hiPSC-NSC-EVs. In RAW-ASC cells, naïve hiPSC-NSC-EVs reduced NLRP3 inflammasome activation and IL-1β and IL-18 release after nigericin stimulation, an effect lost with miR-30e-3p-depleted hiPSC-NSC-EVs. Similarly, in RAW-Lucia-ISG cells, naïve hiPSC-NSC-EVs decreased luciferase activity after cGAMP stimulation, indicating suppressed STING activation, which was absent when miR-181a-5p-depleted hiPSC-NSC-EVs were employed. Overall, multiple miRNAs and proteins within hiPSC-NSC-EVs can reduce microglial proinflammatory responses, with miR-30e-3p and miR-181a-5p specifically linked to inhibition of the NLRP3 inflammasome and the cGAS-STING pathway, respectively. These findings align with previous studies on the roles of these miRNAs (Li et al. 2018; Bustos et al. 2023).

4.5 | Impact of hiPSC-NSC-EVs Treatment in Late Middle Age on Cognitive Function in Old Age

Cognitive and mood impairments are commonly observed in late-middle-aged mice (Frick et al. 2000; Barreto et al. 2010; Radulescu et al. 2021). At 18 months, both male and female mice exhibited deficits in recognition memory (measured by NORT) and object location memory (measured by OLT), which rely on the integrity of the perirhinal cortex and hippocampus (Aggleton et al. 2010; Barker and Warburton 2011). These impairments persisted into old age for vehicle-treated mice. However, male and female mice treated with hiPSC-NSC-EVs showed improved recognition and object-location memory in old age, suggesting that hiPSC-NSC-EVs treatment induced beneficial changes in the hippocampus and other brain regions, thereby reversing cognitive deficits. Since increased oxidative stress and neuroinflammation are linked to cognitive impairments in aging mice (Britton et al. 2022; Morrison and Baxter 2012; Petralia et al. 2014; Bhatt et al. 2009; Holtmaat and Svoboda 2009), the current study suggests that reductions in oxidative stress and neuroinflammatory signalling, mediated by hiPSC-NSC-EVs treatment, have improved cognitive function in old age. This finding aligns with the understanding that neuroinflammation is a risk factor for MCI, dementia, and AD (Walker et al. 2023). However, any positive impact of hiPSC-NSC-EVs on neurons, which may also contribute to better cognitive function in aged mice, requires further investigation. Nonetheless, the current study is the first to demonstrate the beneficial effects of hiPSC-NSC-EVs on cognitive function in aged animals, whereas previous studies using EVs from mesenchymal stem cells have reported other benefits, such as improved locomotor function and neuroprotection (Hao et al. 2025) and microglia-mediated synapse remodelling (Zhou et al. 2023) in aging models.

5 | Conclusion and Limitations

The results indicate that IN administration of hiPSC-NSC-EVs during late middle age can alter the proinflammatory transcriptome within microglia in the aged brain, leading to reduced oxidative stress and neuroinflammaging, along with improved cognitive and memory function. The antiinflammatory effects were demonstrated by decreased activation of several microglia-mediated proinflammatory signalling pathways in the aged hippocampus. Therefore, hiPSC-NSC-EVs treatment in late middle age has promise to help reduce brain inflammation and potentially delay MCI and AD. However, more research is needed before clinical application. Furthermore, although there was no interaction between sex and hiPSC-NSC-EVs treatment, minor sex-specific effects were observed, with female mice receiving hiPSC-NSC-EVs showing increased expression of a gene (*Ndufs6*) and higher concentration of a few proteins (CAT, pIRF3), compared with males, suggesting a need for further investigation into sex-based responsiveness. Future studies should also examine the effects of treatment initiation timing, various doses, and long-term efficacy of hiPSC-NSC-EVs. Additionally, the development of good manufacturing practice protocols for large-scale production and rigorous testing of clinical-grade hiPSC-NSC-EVs in larger animal models is essential for the successful translation of hiPSC-NSC-EVs therapy to older adults or those with MCI.

Author Contributions

Concept: A.K.S. Research design: A.K.S., L.N.M., M.K., S.R., S.A., and R.U. Data collection, analysis, and interpretation: L.N.M., M.K., S.R., S.A., R.U., G.S., B.S., Y.S., S.V.G., V.S.K., J.E.J., P.A.S., A.L., X.R., J.J.C., and A.K.S. Preparation of figure composites: L.N.M., M.K., S.R., S.A., and Y.S. Manuscript writing: L.N.M., M.K., and A.K.S. All authors provided feedback, edits, and additions to the manuscript text and approved the final version of the manuscript.

Acknowledgements

The TEM images of hiPSC-NSC-EVs were taken at the Image Analysis Laboratory, Texas A&M Veterinary Medicine & Biomedical Sciences (RRIS: SCR_0222479).

Funding

This study was supported by grants from the National Institute on Aging (R01AG075440 and 1RF1AG074256 to Ashok K. Shetty).

Ethics Statement

The animal care and experimental procedures were conducted per the animal protocol approved by the Animal Care and the Use Committee (IACUC) of Texas A&M University School of Medicine.

Conflicts of Interest

The authors declared no conflicts of interest.

Data Availability Statement

The data that support the findings of this study are available from the corresponding author upon reasonable request.

References

Ager, R. R., J. L. Davis, A. Agazaryan, F. Benavente, W. W. Poon, and F. M. LaFerla. 2015. "Blurton-Jones M. Human Neural Stem Cells Improve Cognition and Promote Synaptic Growth in Two Complementary Transgenic Models of Alzheimer's Disease and Neuronal Loss." *Hippocampus* 25, no. 7: 813–826.

Aggleton, J. P., M. M. Albasser, D. J. Aggleton, G. L. Poirier, and J. M Pearce. 2010. "Lesions of the Rat Perirhinal Cortex Spare the Acquisition of a Complex Configural Visual Discrimination Yet Impair Object Recognition." *Behavioral Neuroscience* 124, no. 1: 55–68.

Antignano, I., Y. Liu, N. Offermann, and M. Capasso. 2023. "Aging Microglia." *Cellular and Molecular Life Sciences* 80, no. 5: 126.

Attaluri, S., J. Jaimes Gonzalez, M. Kirmani, A. D. Vogel, R. Upadhya, and M. Kodali, et al. 2023. "Intranasally Administered Extracellular Vesicles From Human Induced Pluripotent Stem Cell-Derived Neural Stem Cells Quickly Incorporate Into Neurons and Microglia in 5xFAD Mice." *Frontiers in Aging Neuroscience* 15: 1200445.

Aunan, J. R., W. C. Cho, and K. Soreide. 2017. "The Biology of Aging and Cancer: A Brief Overview of Shared and Divergent Molecular Hallmarks." *Aging Disease* 8, no. 5: 628–642.

Ayyubova, G., M. Kodali, R. Upadhya, et al. 2023. "Extracellular Vesicles From hiPSC-NSCs Can Prevent Peripheral Inflammation-Induced Cognitive Dysfunction With Inflammasome Inhibition and Improved Neurogenesis in the Hippocampus." *Journal of Neuroinflammation* 20, no. 1: 297.

Ayyubova, G., and L. N. Madhu. 2025. "Microglial NLRP3 Inflammasomes in Alzheimer's Disease Pathogenesis: From Interaction With Autophagy/Mitophagy to Therapeutics." *Molecular Neurobiology* 62, no. 6: 7124–7143.

Baik, S. H., S. Kang, W. Lee, H. Choi, S. Chung, and J. I. Kim. 2019. "Mook-Jung I. A Breakdown in Metabolic Reprogramming Causes Microglia

Dysfunction in Alzheimer's Disease." *Cell Metabolism* 30, no. 3: 493–507 e6.

Barker, G. R., and E. C. Warburton. 2011. "When Is the Hippocampus Involved in Recognition Memory?" *Journal of Neuroscience* 31, no. 29: 10721–10731.

Barnett, R. E., D. J. Conklin, L. Ryan, et al. 2016. "Anti-Inflammatory Effects of miR-21 in the Macrophage Response to Peritonitis." *Journal of Leukocyte Biology* 99, no. 2: 361–371.

Barreto, G., T. T. Huang, and R. G. Giffard. 2010. "Age-Related Defects in Sensorimotor Activity, Spatial Learning, and Memory in C57BL/6 Mice." *Journal of Neurosurgical Anesthesiology* 22, no. 3: 214–219.

Bartman, S., G. Coppotelli, and J. M. Ross. 2024. "Mitochondrial Dysfunction: A Key Player in Brain Aging and Diseases." *Current Issues in Molecular Biology* 46, no. 3: 1987–2026.

Baruch, K., A. Deczkowska, E. David, et al. 2014. "Aging. Aging-Induced Type I Interferon Response at the Choroid Plexus Negatively Affects Brain Function." *Science* 346, no. 6205: 89–93.

Bettio, L. E. B., L. Rajendran, and J. Gil-Mohapel. 2017. "The Effects of Aging in the Hippocampus and Cognitive Decline." *Neuroscience and Biobehavioral Reviews* 79: 66–86.

Bhaskar, K., N. Maphis, G. Xu, et al. 2014. "Microglial Derived Tumor Necrosis Factor-Alpha Drives Alzheimer's Disease-Related Neuronal Cell Cycle Events." *Neurobiology of Disease* 62: 273–285.

Bhatt, D. H., S. Zhang, and W. B. Gan. 2009. "Dendritic Spine Dynamics." *Annual Review of Physiology* 71: 261–282.

Blurton-Jones, M., M. Kitazawa, H. Martinez-Coria, et al. 2009. "Neural Stem Cells Improve Cognition via BDNF in a Transgenic Model of Alzheimer Disease." *PNAS* 106, no. 32: 13594–13599.

Britton, R., A. T. Liu, S. V. Rege, et al. 2022. "Molecular and Histological Correlates of Cognitive Decline Across Age in Male C57BL/6J Mice." *Brain Behaviour* 12, no. 9: e2736.

Bustos, M. A., T. Yokoe, Y. Shoji, et al. 2023. "MiR-181a Targets STING to Drive PARP Inhibitor Resistance in BRCA- Mutated Triple-Negative Breast Cancer and Ovarian Cancer." *Cell Bioscience* 13, no. 1: 200.

Cai, J. J. 2019. "scGEAToolbox: A Matlab Toolbox for Single-Cell RNA Sequencing Data Analysis." *Bioinformatics* btz830.

Chen, M., S. Yu, T. van der Sluis, et al. 2024. "cGAS-STING Pathway Expression Correlates With Genomic Instability and Immune Cell Infiltration in Breast Cancer." *NPJ Breast Cancer* 10, no. 1: 1.

da Rocha, J. F., M. L. Lance, R. Luo, et al. 2025. "Protective Exercise Responses in the Dentate Gyrus of Alzheimer's Disease Mouse Model Revealed With Single-Nucleus RNA-Sequencing." *Nature Neuroscience* 28, no. 7: 1546–1561.

de Magalhaes, J. P., M. Stevens, and D. Thornton. 2017. "The Business of Anti-Aging Science." *Trends in Biotechnology* 35, no. 11: 1062–1073.

Dutta, S., and P. Sengupta. 2016. "Men and Mice: Relating Their Ages." *Life Sciences* 152: 244–248.

Eckert, A., L. Huang, R. Gonzalez, H. S. Kim, M. H. Hamblin, and J. P. Lee. 2015. "Bystander Effect Fuels Human Induced Pluripotent Stem Cell-Derived Neural Stem Cells to Quickly Attenuate Early Stage Neurological Deficits After Stroke." *Stem Cells Translational Medicine* 4, no. 7: 841–851.

Edler, M. K., I. Mhatre-Winters, and J. R. Richardson. 2021. "Microglia in Aging and Alzheimer's Disease: A Comparative Species Review." *Cells* 10, no. 5: 1138.

Fan, X., E. G. Wheatley, and S. A. Villeda. 2017. "Mechanisms of Hippocampal Aging and the Potential for Rejuvenation." *Annual Review of Neuroscience* 40: 251–272.

Frick, K. M., L. A. Burlingame, J. A. Arters, and J. Berger-Sweeney. 2000. "Reference Memory, Anxiety and Estrous Cyclicity in C57BL/6NIA Mice Are Affected by Age and Sex." *Neuroscience* 95, no. 1: 293–307.

Fu, Q., J. Li, L. Qiu, et al. 2020. "Inhibiting NLRP3 Inflammasome With MCC950 Ameliorates Perioperative Neurocognitive Disorders, Suppressing Neuroinflammation in the Hippocampus in Aged Mice." *International Immunopharmacology* 82: 106317.

Ge, X., S. Huang, H. Gao, et al. 2016. "miR-21-5p Alleviates Leakage of Injured Brain Microvascular Endothelial Barrier in Vitro Through Suppressing Inflammation and Apoptosis." *Brain Research* 1650: 31–40.

Grimm, A., and A. Eckert. 2017. "Brain Aging and Neurodegeneration: From a Mitochondrial Point of View." *Journal of Neurochemistry* 143, no. 4: 418–431.

Gruel, R., B. Bijnens, J. Van Den Daele, et al. 2024. "S100A8-Dnriched Microglia Populate the Brain of Tau-Seeded and Accelerated Aging Mice." *Aging Cell* 23, no. 5: e14120.

Gulen, M. F., N. Samson, A. Keller, et al. 2023. "cGAS-STING Drives Ageing-Related Inflammation and Neurodegeneration." *Nature* 620, no. 7973: 374–380.

Gurau, F., S. Baldoni, F. Prattichizzo, et al. 2018. "Anti-Senescence Compounds: A Potential Nutraceutical Approach to Healthy Aging." *Ageing Research Reviews* 46: 14–31.

Hahl, P., T. Davis, C. Washburn, J. T. Rogers, and A. Smith. 2013. "Mechanisms of Neuroprotection by Hemopexin: Modeling the Control of Heme and Iron Homeostasis in Brain Neurons in Inflammatory States." *Journal of Neurochemistry* 125, no. 1: 89–101.

Han, D., Z. Yu, W. Liu, et al. 2018. "Plasma Hemopexin Ameliorates Murine Spinal Cord Injury by Switching Microglia From the M1 State to the M2 State." *Cell Death and Disease* 9, no. 2: 181.

Hao, Y., B. Yu, M. Qin, et al. 2025. "Extracellular Vesicles From Antler Blastema Progenitor Cells Reverse Bone Loss and Mitigate Aging-Related Phenotypes in Mice and Macaques." *Nature Aging* 5, no. 9: 1790–1809.

Harry, G. J. 2013. "Microglia During Development and Aging." *Pharmacology & Therapeutics* 139, no. 3: 313–326.

Hattiangady, B., R. Kuruba, and A. K. Shetty. 2011. "Acute Seizures in Old Age Leads to a Greater Loss of CA1 Pyramidal Neurons, an Increased Propensity for Developing Chronic TLE and a Severe Cognitive Dysfunction." *Aging Disease* 2, no. 1: 1–17.

Hattiangady, B., V. Mishra, M. Kodali, B. Shuai, X. Rao, and A. K. Shetty. 2014. "Object Location and Object Recognition Memory Impairments, Motivation Deficits and Depression in a Model of Gulf War Illness." *Frontiers in Behavioral Neuroscience* 8: 78.

Hattiangady, B., and A. K. Shetty. 2012. "Neural Stem Cell Grafting Counteracts Hippocampal Injury-Mediated Impairments in Mood, Memory, and Neurogenesis." *Stem Cells Translational Medicine* 1, no. 9: 696–708.

Hattiangady, B., B. Shuai, J. Cai, T. Coksaygan, and M. S. Rao, and A. K. Shett. 2007. "Increased Dentate Neurogenesis After Grafting of Glial Restricted Progenitors or Neural Stem Cells in the Aging Hippocampus." *Stem Cells* 25, no. 8: 2104–2117.

Hawkins, P. T., and L. R. Stephens. 2015. "PI3K Signalling in Inflammation." *Biochimica et Biophysica Acta* 1851, no. 6: 882–897.

He, X. F., L. L. Li, W. B. Xian, et al. 2021. "Chronic Colitis Exacerbates NLRP3-Dependent Neuroinflammation and Cognitive Impairment in Middle-Aged Brain." *Journal of Neuroinflammation* 18, no. 1: 153.

Hedden, T., and J. D. Gabrieli. 2004. "Insights Into the Ageing Mind: A View From Cognitive Neuroscience." *Nature Reviews Neuroscience* 5, no. 2: 87–96.

Hefendehl, J. K., J. J. Neher, R. B. Suhs, S. Kohsaka, A. Skodras, and M. Jucker. 2014. "Homeostatic and Injury-Induced Microglia Behavior in the Aging Brain." *Aging Cell* 13, no. 1: 60–69.

Holtmaat, A., and K. Svoboda. 2009. "Experience-Dependent Structural Synaptic Plasticity in the Mammalian Brain." *Nature Reviews Neuroscience* 10, no. 9: 647–658.

Ionescu-Tucker, A., and C. W. Cotman. 2021. "Emerging Roles of Oxidative Stress in Brain Aging and Alzheimer's Disease." *Neurobiology of Aging* 107: 86–95.

Islam, M. T. 2017. "Oxidative Stress and Mitochondrial Dysfunction-Linked Neurodegenerative Disorders." *Neurological Research* 39, no. 1: 73–82.

Jimenez-Loygorri, J. I., B. Villarejo-Zori, A. Viedma-Poyatos, et al. 2024. "Mitophagy Curtails Cytosolic mtDNA-Dependent Activation of cGAS/STING Inflammation During Aging." *Nature Communications* 15, no. 1: 830.

Keane, L., I. Antignano, S. P. Riechers, et al. 2021. "mTOR-Dependent Translation Amplifies Microglia Priming in Aging Mice." *Journal of Clinical Investigation* 131, no. 1: e132727.

Kodali, M., S. Attaluri, L. N. Madhu, et al. 2021. "Metformin Treatment in Late Middle Age Improves Cognitive Function With Alleviation of Microglial Activation and Enhancement of Autophagy in the Hippocampus." *Aging Cell* 20, no. 2: e13277.

Kodali, M., L. N. Madhu, R. L. Reger, et al. 2023. "Intranasally Administered Human MSC-Derived Extracellular Vesicles Inhibit NLRP3-p38/MAPK Signaling After TBI and Prevent Chronic Brain Dysfunction." *Brain, Behavior, and Immunity* 108: 118–134.

Kodali, M., T. Megahed, V. Mishra, B. Shuai, B. Hattiangady, and A. K. Shetty. 2016. "Voluntary Running Exercise-Mediated Enhanced Neurogenesis Does Not Obliterate Retrograde Spatial Memory." *Journal of Neuroscience* 36, no. 31: 8112–8122.

Li, D., H. Yang, J. Ma, S. Luo, S. Chen, and Q. Gu. 2018. "MicroRNA-30e Regulates Neuroinflammation in MPTP Model of Parkinson's Disease by Targeting Nlrp3." *Human Cell* 31, no. 2: 106–115.

Liu, X., C. Xu, W. Xiao, and N. Yan. 2023 Sep. "Unravelling the Role of NFE2L1 in Stress Responses and Related Diseases." *Redox Biology* 65: 102819.

Long, J. M., A. N. Kalehua, N. J. Muth, et al. 1998. "Stereological Analysis of Astrocyte and Microglia in Aging Mouse Hippocampus." *Neurobiology of Aging* 19, no. 5: 497–503.

Loving, B. A., M. Tang, M. C. Neal, et al. 2021. "Lipoprotein Lipase Regulates Microglial Lipid Droplet Accumulation." *Cells* 10, no. 2: 198.

Lu, T., Y. Pan, S. Y. Kao, et al. 2004. "Gene Regulation and DNA Damage in the Ageing Human Brain." *Nature* 429, no. 6994: 883–891.

Madhu, L. N., M. Kodali, S. Attaluri, et al. 2021. "Melatonin Improves Brain Function in a Model of Chronic Gulf War Illness With Modulation of Oxidative Stress, NLRP3 Inflammasomes, and BDNF-ERK-CREB Pathway in the Hippocampus." *Redox Biology* 43: 101973.

Madhu, L. N., M. Kodali, R. Upadhya, et al. 2024. "Extracellular Vesicles From Human-Induced Pluripotent Stem Cell-Derived Neural Stem Cells Alleviate Proinflammatory Cascades Within Disease-Associated Microglia in Alzheimer's Disease." *Journal of Extracellular Vesicles* 13, no. 11: e12519.

Miao, J., L. Chen, X. Pan, L. Li, B. Zhao, and J. Lan. 2023. "Microglial Metabolic Reprogramming: Emerging Insights and Therapeutic Strategies in Neurodegenerative Diseases." *Cellular and Molecular Neurobiology* 43, no. 7: 3191–3210.

Morrison, J. H., and M. G. Baxter. 2012. "The Ageing Cortical Synapse: Hallmarks and Implications for Cognitive Decline." *Nature Reviews Neuroscience* 13, no. 4: 240–250.

Mosher, K. I., and T. Wyss-Coray. 2014. "Microglial Dysfunction in Brain Aging and Alzheimer's Disease." *Biochemical Pharmacology* 88, no. 4: 594–604.

Nascimento, E. F. D., P. V. C. Batista, C. S. Cunha, et al. 2025. "Targeting the Dectin-1 Receptor in Neuroinflammation: Therapeutic Implications for Neuropsychiatric Disorders." *ACS Chemical Neuroscience* 16, no. 16: 3082–3095.

Ndoja, A., R. Reja, S. H. Lee, et al. 2020. "Ubiquitin Ligase COP1 Suppresses Neuroinflammation by Degrading c/EBPbeta in Microglia." *Cell* 182, no. 5: 1156–1169 e12.

Nomaru, H., K. Sakumi, A. Katogi, et al. 2014. "Fosb Gene Products Contribute to Excitotoxic Microglial Activation by Regulating the Expression of Complement C5a Receptors in Microglia." *Glia* 62, no. 8: 1284–1298.

Olesen, M. A., A. K. Torres, C. Jara, M. P. Murphy, and C. Tapia-Rojas. 2020. "Premature Synaptic Mitochondrial Dysfunction in the Hippocampus During Aging Contributes to Memory Loss." *Redox Biology* 34: 101558.

O'Shea, A., R. A. Cohen, E. C. Porges, N. R. Nissim, and A. J. Woods. 2016. "Cognitive Aging and the Hippocampus in Older Adults." *Frontiers in Aging Neuroscience* 8: 298.

Pampuscenko, K., S. Jankeviciute, R. Morkuniene, et al. 2025. "S100A9 Protein Activates Microglia and Stimulates Phagocytosis, Resulting in Synaptic and Neuronal Loss." *Neurobiology of Disease* 206: 106817.

Paul, B. D., S. H. Snyder, and V. A. Bohr. 2021. "Signaling by cGAS-STING in Neurodegeneration." *Neuroinflammation, and Aging Trends in Neuroscience* 44, no. 2: 83–96.

Petralia, R. S., M. P. Mattson, and P. J. Yao. 2014. "Communication Breakdown: The Impact of Ageing on Synapse Structure." *Ageing Research Reviews* 14: 31–42.

Radulescu, C. I., V. Cerar, P. Haslehurst, M. Kopanitsa, and S. J. Barnes. 2021. "The Aging Mouse Brain: Cognition, Connectivity and Calcium." *Cell Calcium* 94: 102358.

Raftery, N., and N. J. Stevenson. 2017. "Advances in Anti-Viral Immune Defence: Revealing the Importance of the IFN JAK/STAT Pathway." *Cellular and Molecular Life Sciences* 74, no. 14: 2525–2535.

Rajkovic, I., R. Wong, E. Lemarchand, R. Tinker, S. M. Allan, and E. Pinteaux. 2019. "Pentraxin 3 Regulates Neutrophil Infiltration to the Brain During Neuroinflammation." *AMRC Open Research* 1: 10.

Rao, M. S., B. Hattiangady, K. S. Rai, and A. K. Shetty. 2007. "Strategies for Promoting Anti-Seizure Effects of Hippocampal Fetal Cells Grafted Into the Hippocampus of Rats Exhibiting Chronic Temporal Lobe Epilepsy." *Neurobiology of Disease* 27, no. 2: 117–132.

Rao, M. S., B. Hattiangady, and A. K. Shetty. 2006. "Fetal Hippocampal CA3 Cell Grafts Enriched With FGF-2 and BDNF Exhibit Robust Long-Term Survival and Integration and Suppress Aberrant Mossy Fiber Sprouting in the Injured Middle-Aged Hippocampus." *Neurobiology of Disease* 21, no. 2: 276–290.

Rao, M. S., B. Hattiangady, and A. K. Shetty. 2008. "Status Epilepticus During Old Age Is Not Associated With Enhanced Hippocampal Neurogenesis." *Hippocampus* 18, no. 9: 931–944.

Rao, S., L. N. Madhu, R. S. Babu, et al. 2025. "Extracellular Vesicles From hiPSC-Derived NSCs Protect Human Neurons Against Abeta-42 Oligomers Induced Neurodegeneration, Mitochondrial Dysfunction and Tau Phosphorylation." *Stem Cell Research & Therapy* 16, no. 1: 191.

Rodrigues, M. S., N. B. do Nascimento, H. R. Farias, et al. 2024. "Microglia Contribute to Cognitive Decline in Hypercholesterolemic LDLr(-/-) Mice." *Journal of Neurochemistry* 168, no. 8: 1565–1586.

Seki, T., M. Kanagawa, K. Kobayashi, et al. 2020. "Galectin 3-Binding Protein Suppresses Amyloid-Beta Production by Modulating Beta-Cleavage of Amyloid Precursor Protein." *Journal of Biological Chemistry* 295, no. 11: 3678–3691.

Seok, J. K., M. Kim, H. C. Kang, Y. Y. Cho, H. S. Lee, and J. Y. Lee. 2023. "Beyond DNA Sensing: Expanding the Role of cGAS/STING in Immunity and Diseases." *Archives of Pharmacal Research* 46, no. 6: 500–534.

Shang, Y. C., Z. Z. Chong, J. Hou, and K. Maiese. 2009a. "FoxO3a Governs Early Microglial Proliferation and Employs Mitochondrial Depolarization With Caspase 3, 8, and 9 Cleavage During Oxidant Induced Apoptosis." *Current Neurovascular Research* 6, no. 4: 223–238.

Shang, Y. C., Z. Z. Chong, J. Hou, and K. Maiese. 2009b. "The Forkhead Transcription Factor FOXO3a Controls Microglial Inflammatory Activation and Eventual Apoptotic Injury Through Caspase 3." *Current Neurovascular Research* 6, no. 1: 20–31.

Sheedy, F. J. 2015. "Turning 21: Induction of miR-21 as a Key Switch in the Inflammatory Response." *Frontiers in Immunology* 6: 19.

Shetty, A. K., S. Attaluri, M. Kodali, et al. 2020. "Monosodium Luminol Reinstates Redox Homeostasis, Improves Cognition, Mood and Neurogenesis, and Alleviates Neuro- and Systemic Inflammation in a Model of Gulf War Illness." *Redox Biology* 28: 101389.

Shetty, A. K., and B. Hattiangady. 2016. "Grafted Subventricular Zone Neural Stem Cells Display Robust Engraftment and Similar Differentiation Properties and Form New Neurogenic Niches in the Young and Aged Hippocampus." *Stem Cells Translational Medicine* 5, no. 9: 1204–1215.

Shindo, A., T. Maki, E. T. Mandeville, et al. 2016. "Astrocyte-Derived Pentraxin 3 Supports Blood-Brain Barrier Integrity Under Acute Phase of Stroke." *Stroke; A Journal of Cerebral Circulation* 47, no. 4: 1094–1100.

Silvin, A., S. Uderhardt, and C. Piot, et al. 2022. "Dual Ontogeny of Disease-Associated Microglia and Disease Inflammatory Macrophages in Aging and Neurodegeneration." *Immunity* 55, no. 8: 1448–1465 e6.

Slota, J. A., and S. A. Booth. 2019. "MicroRNAs in Neuroinflammation: Implications in Disease Pathogenesis, Biomarker Discovery and Therapeutic Applications." *Noncoding RNA* 5, no. 2: 35.

Stambler, I. 2017. "Recognizing Degenerative Aging as a Treatable Medical Condition: Methodology and Policy." *Aging Disease* 8, no. 5: 583–589.

Stefanatos, R., and A. Sanz. 2018. "The Role of Mitochondrial ROS in the Aging Brain." *FEBS Letters* 592, no. 5: 743–758.

Terzioglu, G., and Y.-P. TL. 2023. "Microglial Function, INPP5D/SHIP1 Signaling, and NLRP3 Inflammasome Activation: Implications for Alzheimer's Disease." *Molecular Neurodegeneration* 18, no. 1: 89.

Turrini, S., B. Wong, M. Eldaief, et al. 2023. "The Multifactorial Nature of Healthy Brain Ageing: Brain Changes, Functional Decline and Protective Factors." *Ageing Research Reviews* 88: 101939.

Upadhya, R., L. N. Madhu, S. Attaluri, et al. 2020. "Extracellular Vesicles From Human iPSC-Derived Neural Stem Cells: miRNA and Protein Signatures, and Anti-Inflammatory and Neurogenic Properties." *Journal of Extracellular Vesicles* 9, no. 1: 1809064.

Upadhya, R., L. N. Madhu, S. Rao, and A. K. Shetty. 2022. "Proficiency of Extracellular Vesicles From hiPSC-Derived Neural Stem Cells in Modulating Proinflammatory Human Microglia: Role of Pentraxin-3 and miRNA-21-5p." *Frontiers in Molecular Neuroscience* 15: 845542.

Valiukas, Z., K. Tangalakis, V. Apostolopoulos, and J. Feehan. 2025. "Microglial Activation States and Their Implications for Alzheimer's Disease." *Journal of Prevention of Alzheimers Disease* 12, no. 1: 100013.

Viorel, V. I., Y. Pastorello, N. Bajwa, and M. Slevin. 2024. "p38-MAPK and CDK5, Signaling Pathways in Neuroinflammation: A Potential Therapeutic Intervention in Alzheimer's Disease?" *Neural Regeneration Research* 19, no. 8: 1649–1650.

Walker, K. A., L. M. Le Page, N. Terrando, M. R. Duggan, M. T. Heneka, and B. M. Bettcher. 2023. "The Role of Peripheral Inflammatory Insults in Alzheimer's Disease: A Review and Research Roadmap." *Molecular Neurodegeneration* 18, no. 1: 37.

Wang, X., G. Chen, and B. Wan, et al. 2022. "NRF1-Mediated Microglial Activation Triggers High-Altitude Cerebral Edema." *Journal of Molecular Cell Biology* 14, no. 5: mjac036.

Wang, Y., T. Wu, and M. C. Tsai, et al. 2023. "TPL2 Kinase Activity Regulates Microglial Inflammatory Responses and Promotes Neurodegeneration in Tauopathy Mice." *eLife* 12: e83451.

Wei, A., B. Liu, Y. Li, et al. 2025. "Rap1a Regulates CUMS-Induced Neuroinflammation and Cognitive Dysfunction and Emotional Abnormalities in Mice." *International Immunopharmacology* 165: 115483.

Wolf, S. A., H. W. Boddeke, and H. Kettenmann. 2017. "Microglia in Physiology and Disease." *Annual Review of Physiology* 79: 619–643.

Wu, L., Y. Li, M. Yu, F. Yang, M. Tu, and H. Xu. 2018. "Notch Signaling Regulates Microglial Activation and Inflammatory Reactions in a Rat Model of Temporal Lobe Epilepsy." *Neurochemical Research* 43, no. 6: 1269–1282.

Yang, H., H. Wang, Y. Shu, and X. Li. 2018. "miR-103 Promotes Neurite Outgrowth and Suppresses Cells Apoptosis by Targeting Prostaglandin-Endoperoxide Synthase 2 in Cellular Models of Alzheimer's Disease." *Frontiers in Cell Neuroscience* 12: 91.

Yu, W. H., L. Go, B. A. Guinn, P. E. Fraser, D. Westaway, and J. McLaurin. 2002. "Phenotypic and Functional Changes in Glial Cells as a Function of Age." *Neurobiology of Aging* 23, no. 1: 105–115.

Zhang, T., C. Wang, Y. Li, et al. 2025. "Lipocalin-2 Induces Macrophage/Microglia Pro-Inflammatory Phenotype After Intracerebral Hemorrhage via Nrf2 Signaling Inhibition in Young and Aged Mice." *Neuroscience Research* 222: 104988.

Zhou, C., H. Chen, J. F. Zheng, et al. 2020. "Pentraxin 3 Contributes to Neurogenesis After Traumatic Brain Injury in Mice." *Neural Regeneration Research* 15, no. 12: 2318–2326.

Zhou, Y., H. Bhatt, C. A. Mojica, et al. 2023. "Mesenchymal-Derived Extracellular Vesicles Enhance Microglia-Mediated Synapse Remodeling After Cortical Injury in Aging Rhesus Monkeys." *Journal of Neuroinflammation* 20, no. 1: 201.

Supporting Information

Additional supporting information can be found online in the Supporting Information section.

Supporting Information: jev270232-sup-0001-SuppMat.docx